

MODAL ANALYSIS FOR SMALL ENGINE CRANKSHAFT

SANTHANA JULIAS A/L HENRY

BACHELOR OF ENGINEERING
UNIVERSITI MALAYSIA PAHANG

2010

MODAL ANALYSIS FOR SMALL ENGINE CRANKSHAFT

SANTHANA JULIAS A/L HENRY

A thesis submitted in fulfillment of the
requirements for the award of the degree of
Bachelor of Mechanical Engineering with Automotive Engineering

Faculty of Mechanical Engineering
University Malaysia Pahang

NOVEMBER 2010

UNIVERSITI MALAYSIA PAHANG
FACULTY OF MECHANICAL ENGINEERING

We certify that the project entitled “Modal Analysis For Small Engine Crankshaft” is written by Santhana Julias A/l Henry. We have examined the final copy of this project and in our opinion; it is fully adequate in terms of scope and quality for the award of the degree of Bachelor of Engineering. We herewith recommend that it be accepted in partial fulfillment of the requirements for the degree of Bachelor of Mechanical Engineering with Automotive Engineering.

MR. CHE KU EDDY NIZWAN CHE KU HUSIN

Examiner

Signature

SUPERVISOR'S DECLARATION

I hereby declare that I have checked this project and in my opinion, this project is adequate in terms of scope and quality for the award of the degree of Bachelor of Mechanical Engineering with Automotive Engineering.

Signature:

Name of Supervisor: MR. MOHD FIRDAUS BIN HASSAN

Position: LECTURER

Date: 6th DECEMBER 2010

STUDENT'S DECLARATION

I hereby declare that the work in this thesis is my own except for quotations and summaries which have been duly acknowledged. The thesis has not been accepted for any degree and is not concurrently submitted for award of other degree.

Signature:

Name: SANTHANA JULIAS A/L HENRY

ID Number: MH08085

Date: 6th DECEMBER 2010

DEDICATION

Dedicated to my beloved

parents and friends

for their support and motivation that they gave

while working on this thesis

ACKNOWLEDGEMENT

I am grateful and would like to express my sincere gratitude to my supervisor Mr. Mohd Firdaus Hassan for his germinal ideas, invaluable guidance, continuous encouragement and constant support in making this research possible. He has always impressed me with his outstanding professional conduct, his strong conviction for science. I appreciate his consistent support from the first day I applied to graduate program to these concluding moments. I am truly grateful for his progressive vision about my training in science, his tolerance of my naïve mistakes, and his commitment to my future career. I also would like to express very special thanks to DR Daw Thet Thet Mon for her suggestions and co-operation throughout the study. I also sincerely thanks for the time spent proofreading and correcting my many mistakes.

My sincere thanks go to members of the staff of the Mechanical Engineering Department, UMP, who helped me in many ways and made my stay at UMP pleasant and unforgettable.

I acknowledge my sincere indebtedness and gratitude to my parents for their love, dream and sacrifice throughout my life. They also consistently encouraged me to carry on my higher studies in UMP. I cannot find the appropriate words that could properly describe my appreciation for their devotion, support and faith in my ability to attain my goals. Special thanks should be given to my committee members. I would like to acknowledge their comments and suggestions, which was crucial for the successful completion of this study.

Thank you.

ABSTRACT

This thesis consists of finding the mode shape and natural frequency of a 4 stroke motorcycle engine crankshaft. The test is done in both simulation and also experimental using a simple test rig. The crankshaft is modeled using Solidworks computer aided design (CAD) software and simulation analysis is done in ALGOR computational aided engineering (CAE) software. Experimental is done by using impact hammer to excite the crankshaft and data recorded using data acquisition system (DAS) connected to sensor located on the crankshaft. The results for both simulation and experimental is compared. The final selected natural frequency for simulation is based on mesh aspect ratio of 60%. Simulation natural frequency in 1st mode is 1044.9 Hz (bending in face off), 2nd mode is 1204.59 Hz (bending in face axis), 3rd mode is 2104.59 Hz (bending out of face), 4th mode is 2174.66 Hz (bending out of face) and 5th mode is 2624.24 Hz (bending out of face). Meanwhile, the experimental natural frequency in 1st mode is 990.01 Hz, 2nd mode is 1244 Hz, 3rd mode is 2084.89 Hz, 4th mode is 2219.11 Hz and 5th mode is 2791.18 Hz.. The discrepancy errors recorded between simulation and experimental is ranging from 0.94 – 6.56 %.

ABSTRAK

Tesis ini terdiri dalam mencari bentuk mod dan frekuensi semulajadi aci engkol sebuah enjin motorsikal 4 lejang. Ujian ini dijalankan dalam dua keadaan iaitu eksperimen dan simulasi komputer. Aci engkol akan dimodelkan menggunakan perisian CAD SOLIDWORKS dan analisis simulasi akan dilakukan didalam perisian CAE ALGOR. Eksperimen pula akan dilakukan menggunakan tukul impak untuk menggetarkan aci engkol tersebut. Data akan direkod menggunakan alat pengumpulan data dimana ia disambungkan pada sensor yang terletak pada permukaan aci engkol tersebut. Keputusan yang diperolehi dari kedua-dua eksperimen dan simulasi akan dibandingkan. Nilai frekuensi jati yang muktamad dipilih dari nisbah mesh 60%. Cadangan untuk mempertingkatkan lagi kualiti eksperimen dan simulasi di masa hadapan juga telah disenaraikan. Frekuensi semulajadi secara simulasi pada mod 1 ialah 1059.6 Hz, mod 2 ialah 1204.59 Hz, mod 3 ialah 2104.59 Hz, mod 4 ialah 2174.66 Hz dan mod 5 ialah 262.24 Hz. Frekuensi semulajadi secara eksperimen pada mod 1 ialah 990.01 Hz, mod 2 ialah 1224 Hz, mod 3 ialah 2084.89 Hz, mod 4 ialah 2219.11 Hz dan mod 5 ialah 2791.18 Hz. Peratus ralat yang telah direkodkan berada dalam lingkungan 0.94 – 6.56 %.

TABLE OF CONTENTS

	Page
TITLE	i
EXAMINER DECLARATION	ii
SUPERVISOR DECLARATION	iii
STUDENT DECLARATION	iv
ACKNOWLEDGEMENTS	v
ABSTRACT	vi
ABSTRAK	vii
TABLE OF CONTENTS	viii
LIST OF TABLES	xii
LIST OF FIGURES	xiii
LIST OF SYMBOLS	xvi
LIST OF ABBREVIATION	xvii
CHAPTER 1 INTRODUCTION	
1.1 Introduction	1
1.1.1 Project Background	2
1.2 Problem Statement	4
1.3 Objectives	5
1.4 Scopes of Study	5
CHAPTER 2 LITERATURE REVIEW	
2.1 Introduction	6
2.2 Modal Analysis	7
2.3 Modal Testing	8

2.4	Experimental Modal Analysis	9
2.4.1	Stress Analysis and Optimization of Crankshafts Subject to Dynamic Loading	10
2.4.2	Experimental Modal Analysis	11
2.4.3	New Tools for Structural Testing, Using Impact Hammers and Acceleration	12
2.4.4	Vibration Analysis Based On Hammer Impact Test for Multilayer Fouling Detection	14
2.5	Finite Element Analysis	15
2.5.1	Modal Analysis and Experiments for Engine Crankshaft	15
2.5.2	A Crankshaft System Model for Structural Dynamic Analysis of Internal Combustion Engines	17
2.5.3	The Influence of Finite Element Meshes on The Results of a Spatial Polycrystalline Aggregate Model	18

CHAPTER 3 METHODOLOGY

3.1	Introduction	20
3.2	Project Flow Chart	21
3.2.1	Process Flow Description	22
3.3	Material Testing	23
3.3.1	Determination of Material Composition	23
3.3.2	Identifying the Material of the Crankshaft	25
3.4	Develop and Modeling the Crankshaft	28
3.5	Finite Element Analysis	30
3.5.1	Analysis Type	30
3.5.2	Element Type	31
3.5.3	Material Properties	32
3.6	Experimental Modal Analysis	33
3.6.1	Introduction about Pulse	33
3.6.2	List of Apparatus	34
3.6.3	Experiment Setup	36

CHAPTER 4 RESULT AND DISCUSSION

4.1	Introduction	38
4.2	Finite Element Model	38
	4.2.1 First Simulation	38
4.3	Simulation Result	40
4.4	Influence Element or Mesh Type	41
4.5	Experimental Result	42
4.6	Grid-Point Natural Frequency	42
	4.5.1 First Point	43
4.7	Coherence Function	45
4.8	Comparison on Experimental and Simulation	46
4.9	Summary of Result	49
	4.9.1 Discussion on Graph of Natural Frequency versus Mesh Size	49
	4.9.2 Discussion on Graph of Mesh Size versus Mesh Aspect Ratio	50
	4.9.3 Discussion Comparison Between Simulation and Experiment	51
4.8	Overall Discussion	51
4.9	Justification from the Result	52

CHAPTER 5 CONCLUSION AND RECOMMENDATION

5.1	Introduction	53
5.2	Summary	53
5.3	Conclusions	54
5.4	Recommendations	54

REFERENCES	56
-------------------	----

APPENDICES	58
-------------------	----

LIST OF TABLES

Table No.	Title	Page
2.1	The number of element in the model	19
3.1	Composition material of crankshaft	25
3.2	Material Properties	27
3.3	List of apparatus	34
4.1	Frequency of 1 st simulation	40
4.2	Mode shape and Frequency in different mesh aspect ratio	40
4.3	Element Type and Final Mesh Ratio	41
4.4	Value of Natural Frequency in different Mode Shape at point 1	43
4.5	Result of Experimental Modal Analysis (Impact Hammer Test)	44
4.6	Average Result of Experimental Modal Analysis (Impact Hammer Test)	44
4.7	Comparison on experimental and simulation data, mode shapes from experiment with mode shapes from simulation at 100% aspect mesh ratio	46
4.8	Comparison on experimental and simulation data, mode shapes from experiment with mode shapes from simulation at 90% aspect mesh ratio	47
4.9	Comparison on experimental and simulation data, mode shapes from experiment with mode shapes from simulation at 80% aspect mesh ratio	47
4.10	Comparison on experimental and simulation data, mode shapes from experiment with mode shapes from simulation at 70% aspect mesh ratio	48
4.11	Comparison on experimental and simulation data, mode shapes from experiment with mode shapes from simulation at 60% aspect mesh ratio	48

LIST OF FIGURES

Figure No.	Page
1.1 Engine crankshaft (motorcycle)	3
2.1 Model of a crankshaft used	10
2.2 Flexible body modes	11
2.3 Impact testing	11
2.4 Shaker test setup	12
2.5 Impact testing setup for the acceleration rate sensor and the accelerometer	13
2.6 Linear spectrum of an accelerometer signal (top trace) and acceleration rate sensor signal (bottom trace).	13
2.7 Sketch of the experimental set-up with	14
2.8 Mode shapes and frequency of a four cylinder crankshaft	16
2.9 Mode shapes and frequency of a six cylinder crankshaft	17
2.10 The finite element mesh for the pulley, crankshaft, flex plate system the PV6 engine	18
3.1 Project flow chart	21
3.2 Spectro Meter	23
3.3 Chosen Flat Surface	24
3.4 Polishing Machine	24
3.5 First Part Modeling in Solid work	29
3.6 Second Part Modeling in Solid work	29
3.7 Third Part Modeling in Solid work	29
3.8 Completed crankshaft Assembly	29
3.9 Analysis Type	30
3.10 Model Mesh Setting	31
3.11 Model after Complete Meshing	32
3.12 Element Material Specification	33
3.13 Impact hammer used in experimental	35
3.14 The data acquisition system	35
3.15 Single-Axial Accelerometer	35

3.16	Impact Hammer Testing Setup	36
4.1	Mesh Model for First Simulation	39
4.2	Mode Shape 1	39
4.3	Mode Shape 2	39
4.4	Mode Shape 3	39
4.5	Mode Shape 4	39
4.6	Mode Shape 5	39
4.7	Frequency measured at point 1	43
4.8	FRF at Point 6	45
4.9	Coherence at Point 6	45
4.10	Graph of Natural Frequency vs % Mesh Size	49
4.11	Graph of Mesh Size vs Mesh Aspect Ratio	50

LIST OF ABBREVIATIONS

CAD	Computer Aided Design
CAE	Computer Aided Education
DAS	Data Acquisition System
DOF	Degree Of Freedom
EMA	Experimental Modal Analysis
ERA	Eigensystem Realisation Algorithm
FEA	Finite Element Analysis
FRF	Frequency Response Feedback
FYP	Final Year Project
ICE	Internal Combustion Engine
MIMO	Multiple Input Multiple Output
SIMO	Single Input Multiple Output

LIST OF APPENDICES

Appendix		Page
A	Simulation Result In Different Mesh Size	58
B	Experiment Results at Different Point on Crankshaft	66
C	Procedures To Run The Pulselab Software	74
D	Gantt chart FYP 1 and FYP 2	79

CHAPTER 1

INTRODUCTION

1.1 INTRODUCTION

Since 1335, the theory of automobile had been recorded, from the first to be driven by wind to the latest state of the art electric vehicle. In 1876, Nicolaus August Otto invented the first internal combustion engine known as The Otto Cycle Engine. Then in 1886, Gottlieb Daimler improved the idea of internal combustion engine that is practical to be used as an automotive engine. Since then, the idea of internal combustion engine had improved exponentially but, the very basic concept of Otto cycle still remains.

In Otto cycle engine or Internal Combustion Engine (ICE), a piston, or series of it will reciprocate in a linear manner, for example, ups and downs. Such linear motion need to be translated into rotational motion in order for the power generated from the movement of the piston into any mechanism that can move the car. The mechanical part that translates all the piston's linear motions is called crankshaft.

Wiiard W. Pulkabek, (2004) said that, in modern ICE, the crankshaft can rotate up to 20000 rpm. At 20000 rpm, with forces exceeds 3000 N push down on the crankshaft, careful consideration of material and calculations is needed to create a crankshaft that can take not only directional forces, but also rotational motion. As the crankshaft rotates, vibration will occurs. The crankshaft working cycles will be shortened dramatically if the vibration is not contained. Frequency of vibration will often occur when a system is vibrating, in this case, the crankshaft.

In ICE, every part has its own natural frequency. Natural frequency is the frequency at which a system naturally vibrates once it has been set into motion. In other words, natural frequency is the number of times a system will oscillate (move back and forth) between its original position and its displaced position, if there is no outside interference. If the crankshaft vibrating frequency is near or same as its natural frequency, resonance will happen and the effect on the crankshaft or even the ICE itself is catastrophic.

1.1.1 Project Background

Crankshaft is a fundamental and a very crucial part in ICE. Its role as the main translational-rotational converter have been used and perfected as early as 1226 by Al-Jazari in his water pump machines. Typically in an ICE, the crankshaft would be fitted with flywheel in order to reduce the pulsating of sudden force exerted during combustion. Without the flywheel, the crankshaft will experience even higher pulsating and thus, increase the crankshaft wear and tear in the crankshaft structure.



Figure 1.1: Engine crankshaft (motorcycle)

Another major problem when dealing with crankshaft is its out-of-balance characteristics. From the figure above, we can see that the crank pins is off from the center, will surely will act as an out-of-balance mass. With the crankshaft is out of balance, it will vibrate when the crankshaft rotate. Frequency will be generated when the crankshaft rotates and if the crankshaft rotating frequency is equal to its natural frequency, resonance will happen and the crankshaft will break in the long term.

Crankshaft in modern ICE normally had been fitted with a counter-balance mass just opposite to compensate with the mass of crank pins. Even though this works amazingly well, it is really impossible to contain all the vibration on the crankshaft, and thus resonance can still happens.

1.2 PROBLEM STATEMENTS

In early era which is the usage of a crankshaft is limited, wood is the most favorable material to be used. Later, when crankshaft became one of the most important parts of machinery, steel have been used. The most commonly used is cast ductile iron, as it is easy to manufacture and easily available at a low price compared to the more advanced forged steel.

Material selection is important as it affects the crankshaft performance, for example, a normal road car engine typically used a cast iron crankshaft, with an optimal torque to be at around 3000-4000 rpm, the crankshaft need to be fabricates so that resonance would not occur during those working conditions. On the other hand, a higher rpm engine with optimal torque output at around 6000-8000 rpm or even higher, material such as forged steel have been seen used. Furthermore, extreme applications such as F1 engine crankshaft which normally operates exceeds 18000 rpm, material such as 4340 VAR Electric Arc Vacuum Re-melt Chrome-Moly Alloy steel have been used.

The selection of material will affect the natural frequency of the crankshaft. Proper selection is needed to avoid resonance in the crankshaft, which in this case, whirling. Whirling can affect the crankshaft's life and engine performance. Whirling causes the crankshaft to deflect, and when crankshaft is deflected, even in micron meters, not only shorten its life but also reduced the engine power output.

In ICE, the crankshaft will likely to fracture when experienced excessive vibration in a long term period. Possible types of failure that normally occurs in crankshaft including shearing and bending and possible breaking. This vibration normally gets bad during resonance which the crankshaft vibration amplitude will vibrate at its peak limit. Resonance will happen when the crankshaft vibration oscillates at its own natural frequency.

1.3 PROJECT OBJECTIVES

The main objective for this project is to identify the dynamic behavior of a small crankshaft (motorcycle) with finding the natural frequency, ω_n and mode shapes.

1.4 PROJECT SCOPES

The scopes for this project are:

- a) To identify a small crankshaft that to be used
- b) Determine the properties of the crankshaft
- c) Modeling of the crankshaft using solidwork
- d) Performing FEA use Algor software
- e) Performing modal analysis test using impact hammer
- f) Comparison between simulation and experimental.

CHAPTER 2

LITERATURE REVIEW

2.1 INTRODUCTION

In real life application and testing, experimental modal analysis is a crucial and accurate method to find the natural frequency and mode shape, but it is a very time consuming method especially on a large object such as a bridge or a steel tower like The Eiffel Tower in France. Finding these objects mode shapes and natural frequency can take weeks or even months to complete. This is where Finite Element Analysis comes in handy.

Finite Element Analysis or better known as FEA has been developed in 1943 by Richard Courant, who used the Ritz method of numerical analysis and minimization of variational calculus to obtain approximate solutions to vibration systems. From the engineering side, the finite element analysis originated as the displacement method of the matrix structural analysis, which emerged over the course of several decades mainly in British aerospace research as a variant suitable for computers. By late 1950s, the key concepts of stiffness matrix and element assembly existed essentially in the form used today and NASA issued request for proposals for the development of the finite element software NASTRAN in 1965.

2.2 MODAL ANALYSIS (MA)

Modal Analysis (Jimin He and Zhi-Fang Fu, 2001) is the process of determining the inherent dynamic characteristics of a system in forms of natural frequencies. Damping factors and mode shapes, and using them to formulate a mathematical model for its dynamic behavior. The formulated mathematical model is referred to as the modal model of the system and the information for the characteristics are known as its modal data.

The dynamics of a structure are physically decomposed by frequency and position. This is clearly evidenced by the analytical solution of partial differential equations of continuous systems such as beam and strings. Modal analysis is based upon the fact that the vibration response of the linear time invariant dynamic system can be expressed as linear combination of a set of simple harmonic motions called the natural modes of vibration. This concept is akin to the use of a Fourier combination of sine and cosine waves to represent a complicated waveform. The natural modes of vibration are inherent to a dynamic system and are determined completely by its physical properties (mass, stiffness, damping) and their spatial distribution. Each mode is described in term of its modal parameter: natural frequency, the modal factor and characteristic displacement pattern, namely mode shape. The mode shape may be real or complex. Each corresponds to a natural frequency. The degree of participation of each natural mode in the overall vibration is both determined by properties of the excitation source(s) and by the mode shapes of the system.

Modal analysis embraces both theoretical and experimental techniques. The theoretical modal analysis anchors on a physical model of a dynamic system comprising its mass, stiffness and damping properties. These properties may be given in forms of partial differential equation. An example is wave equation of a uniform vibratory string established from its mass distribution and elasticity properties. The solution of the equation provides the natural frequencies and mode shapes of the string and its force vibration responses. However, a more realistic physical model will usually comprise the mass, stiffness and damping properties in terms of their

spatial distributions, namely the mass, stiffness and damping matrices. These matrices are incorporated into a set of normal differential equation of motion the superposition principle of a linear dynamic system enables us to transform these equation into a typical Eigen value problem. Its solution provides the modal data of the system. Modal finite element analysis empowers the discretization of almost any linear dynamic structure and linear dynamic structure and hence has greatly enhanced the capacity and scope of theoretical modal analysis .On the other hand, the rapid developed over the last two decades of data acquisition and processing capabilities has given to major advance in the experimental realm of the analysis which has become known as modal testing.

2.3 MODAL TESTING

Modal testing is an experimental technique used to derive the modal model of a linear time-invariant vibratory system. The theoretical basis of the technique is secured upon establishing the relationship between the vibration response at one location and excitation at the same or another location as a function of excitation frequency. This relationship, which is often a complex mathematical function, is known as frequency response function or FRF in short. Combination of excitation and response at different location lead to a complete set of frequency functions (FRFs) which can be collectively represented by and FRF an FRF matrix of the system. This matrix is usually symmetric, reflecting the structural of the system.

The practice of modal testing involves measuring the FRFs or impulse responses of a structure. The FRF measurement can simply be done by asserting a measured excitation at one location of the structure in the absence of other excitation and measure vibration responses at one or more location. Modern excitation technique and recent developments modal analysis theory permit more complicated excitation mechanisms. The excitation can be of a selected frequency band, stepped sinusoid, transient, random or white noise. It is usually measured by a force transducer at the driving point while the response is measured by accelerometer or other probes. Both the excitation and response signals are fed into an analyzer which is an instrument responsible for computing the FRF data.

A practical consideration of modal testing is how much FRF data need to be acquired in order to adequately derive the modal model of the tested object. When doing a simple hammer test, a fixed response location is used while alternately moving force excitation points. The measured FRF data constitute a row of the FRF matrix. These data would theoretically suffice for deriving the modal model. For a simple shaker test, a fixed force input location is used while alternately moving response collection points or simultaneously acquiring responses from points. The measured FRF data constitute a column of the FRF matrix. Again, the data should suffice theoretically. With sufficient data, numerical analysis will derive modal parameters by ways of curve fitting .this process is known as experimental modal analysis. The derived parameters will form the modal model for test structure. Parameter can be extracted either from individual FRF curves or form a set of FRF curves.

In summary, experimental modal analysis involves three constituent phases test preparation, frequency response measurements and modal parameter identification. Test preparation involves selection of a structure's support, support, type of excitation force, and location of excitation. Hardware to measure force and responses, determination of a structural geometry model which consists of points of response to be measured, and identification of mechanisms which could lead to inaccurate measurement .during the test, a set of FRF data is measured and stored which is then analyzed to identify modal parameters of the tested structure.

2.4 EXPERIMENTAL MODAL ANALYSIS (EMA)

Modal Analysis, or more accurately Experimental Modal Analysis, is the field of measuring and analyzing the dynamic response of structures and or fluids when excited by an input. Examples would include measuring the vibration of a car's body when it is attached to an electromagnetic shaker, or the noise pattern in a room when excited by a loudspeaker. Classically this was done with a SIMO approach, Single Input, Multiple Output, that is, one excitation point, and then the response is measured at many other points. However in recent years MIMO has become more practical.

Typical excitation signals can be classed as impulse, broadband, swept sine, chirp, and possibly others. Each has their own advantages and disadvantages. The analysis of the signals typically relies on Fourier analysis. The resulting transfer function will show one or more resonances, whose characteristic mass, frequency and damping can be estimated from the measurements.

2.4.1 Stress Analysis and Optimization of Crankshafts Subject to Dynamic Loading

Halderman and Mitchell (2001) in his research shows about the weight and cost reduction opportunities for a forged steel crankshaft. The need of load history in the FEM analysis necessitates performing a detailed dynamic load analysis. Therefore, this study consists of three major sections:

- (1) Dynamic load analysis
- (2) FEM and stress analysis
- (3) Optimization for weight and cost reduction.

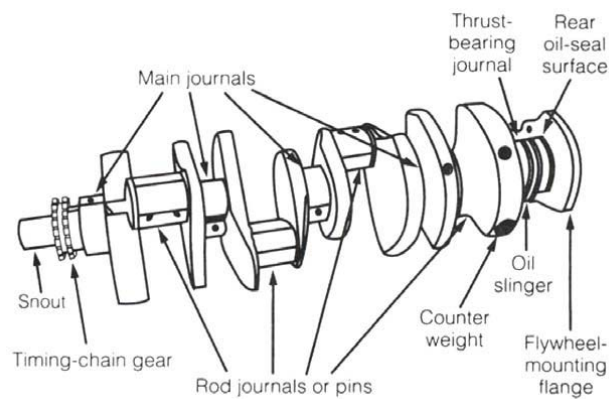


Figure 2.1: Model of a crankshaft used

Source: Halderman and Mitchell, 2001

2.4.2 Experimental Modal Analysis

In this research Brian J. Schwarz & Mark H (2009) presents the fundamental of experimental modal analysis. The investigation are been done using impact hammer and stroke hammer. The objective is to investigate the relation of modes in modal analysis.

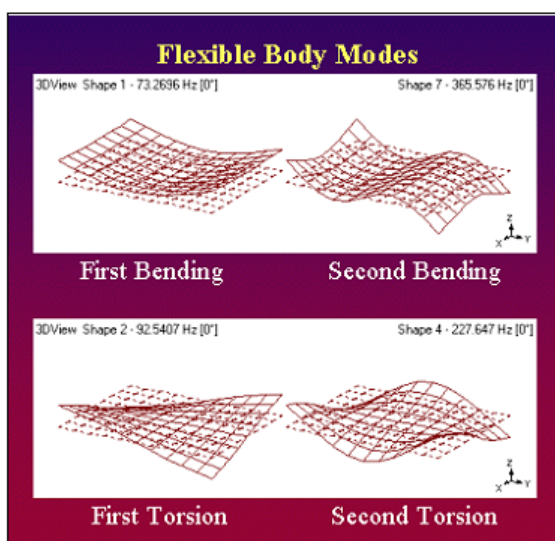


Figure 2.2: Flexible body modes

Source: Brian J. Schwarz & Mark H. Richardson, 1999

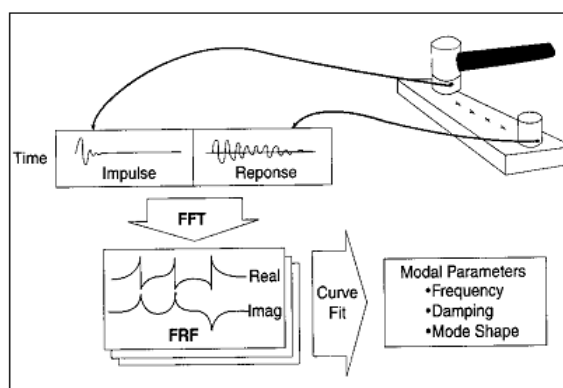


Figure 2.3: Impact testing

Source: Brian J. Schwarz & Mark H. Richardson 1999

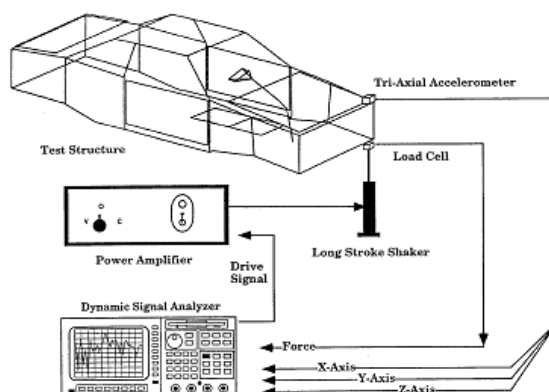


Figure 2.4: Shaker test setup

Source: Brian J. Schwarz & Mark H. Richardson, 1999

2.4.3 New Tools for Structural Testing: Piezoelectric Impact Hammers and Acceleration Rate Sensors

Beside that, C. K. Lee et al., (1998) They also said in their research that Small-size ultra-high-precision mechanical systems demand special testing methodologies, such as a better high frequency response, a precise impact position, and an extremely high repeatability. Utilizing the fact that signals obtained from piezoelectric sensing elements are strongly influenced by the interfacing circuitry, piezoelectric sensors that can be used to measure acceleration rate were developed. Both analytical and experimental results indicate that acceleration rate sensors can detect the arrival of realistic shock earlier than conventional accelerometers. An ultra-high-precision high-speed piezoelectric impact system with an on-line load cell was also modeled, designed, and built. The sensitivity of this on-line load cell was calibrated by using a standard quartz load cell. This innovative high-speed impact hammer system was found to have a timing accuracy in the range of microseconds and a positioning accuracy in the range of micrometers

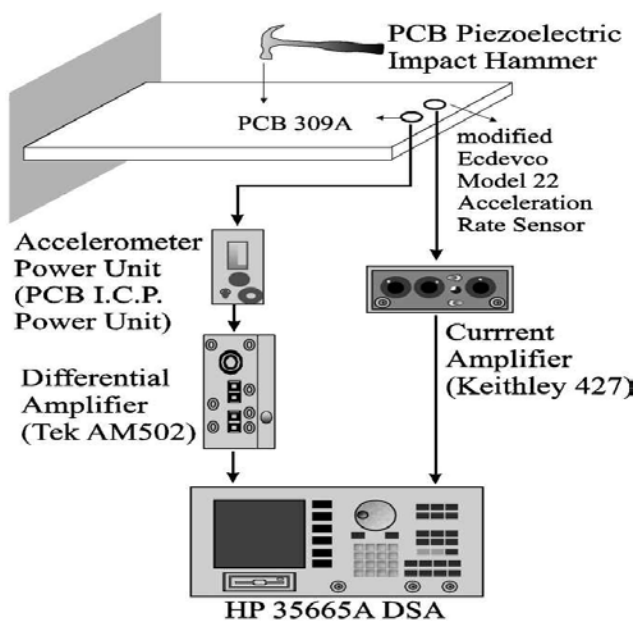


Figure 2.5: Impact testing setup for the acceleration rate sensor and the accelerometer.

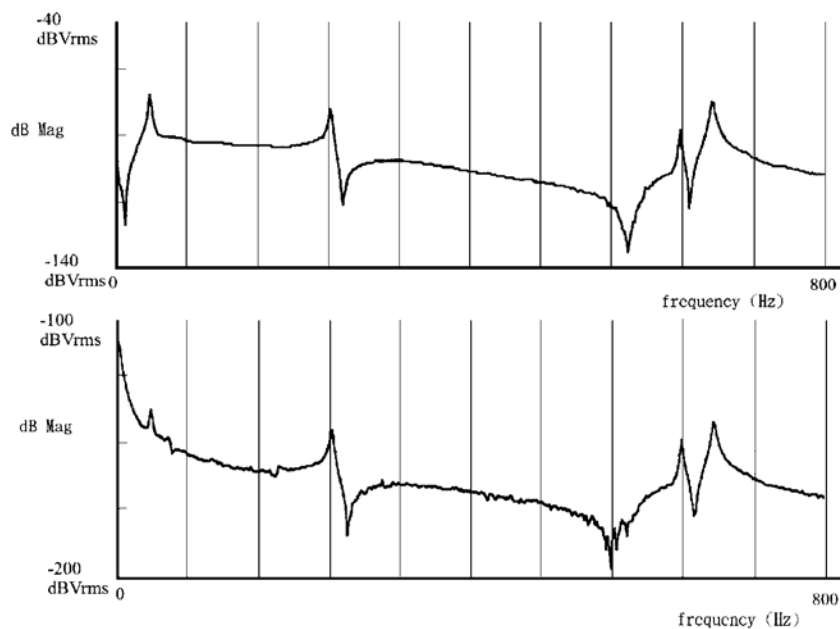


Figure 2.6: Linear spectrum of an accelerometer signal (top trace) and acceleration rate sensor signal (bottom trace).

Source: C. K. Lee, et al., 1998

2.4.4 Vibration Analysis Based On Hammer Impact Test for Multilayer Fouling Detection

Furthermore, Jaidilson Jo da Silva, et al., (2009) also states that the easy detection of fouling in duct systems is a persistent problem and remains a relevant demand for the chemical, oil, food and pharmaceutical industries. This work presents preliminary research results of vibrational hammer excitation for easy to use external non-invasive, nondestructive multi-layer fouling detection in pipelines and other large scale duct systems. Data were taken from the vibration amplitude and frequency variation in presence of an inner pipe fouling layer using acoustic accelerometer and microphone detection.

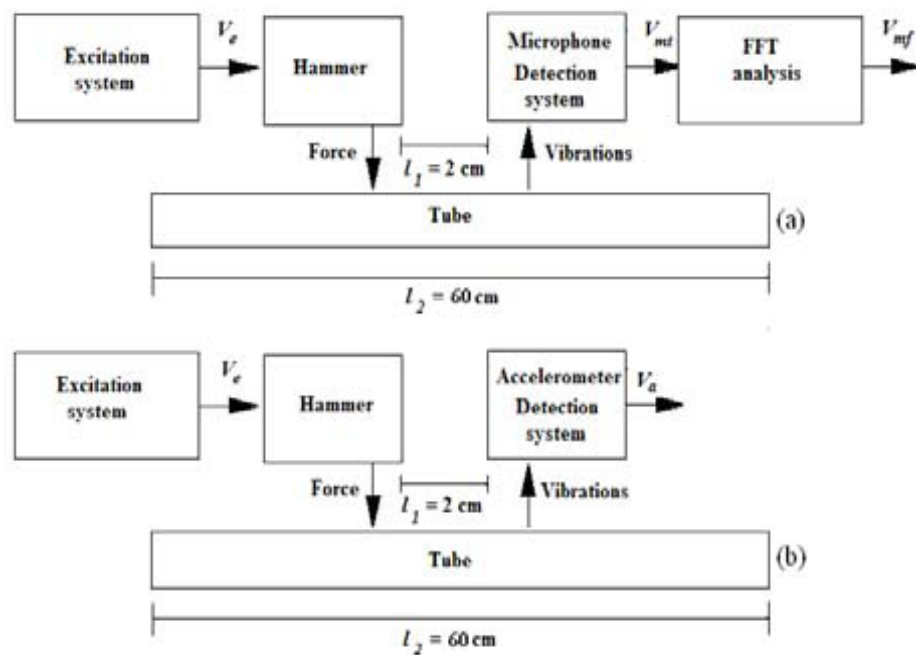


Figure 2.7: Sketch of the experimental set-up with: (a) hammer and
(b) accelerometer

Source: Jaidilson Jo da Silva, et al., 2009

2.5 FINITE ELEMENT ANALYSIS (FEA)

Finite element analysis (FEA) is a computer simulation technique used in engineering analysis. It uses a numerical technique called the finite element method (FEM). Development of the finite element method in structural mechanics is usually based on an energy principle such as the virtual work principle or the minimum total potential energy principle.

The finite element analysis from the mathematical side was first developed in 1943 by Richard Courant,(1993) who used the Ritz method of numerical analysis and minimization of variational calculus to obtain approximate solutions to vibration systems. From the engineering side, the finite element analysis originated as the displacement method of the matrix structural analysis, which emerged over the course of several decades mainly in British aerospace research as a variant suitable for computers. By late 1950s, the key concepts of stiffness matrix and element assembly existed essentially in the form used today and NASA issued request for proposals for the development of the finite element software NASTRAN in 1965.

2.5.1 Modal Analysis and Experiments for Engine Crankshaft

In other research, Y.Kang, et al.,(1997) they studies on investigates the coupled modes including coupled torsional flexural vibration and coupled longitudinal flexural vibration for non rotating crankshafts which are free boundary condition. The finite element models of those generally used are in two categories, which are beam elements and solid elements. By using these two models the natural frequencies and mode shapes of two crankshafts are determined by the finite element method (FEM) and compared with experimental data from modal testing. The accuracy and validity of the analytical approaches are verified. The results show that the solid element is more appropriate than the beam element in the modal analysis of crankshafts.

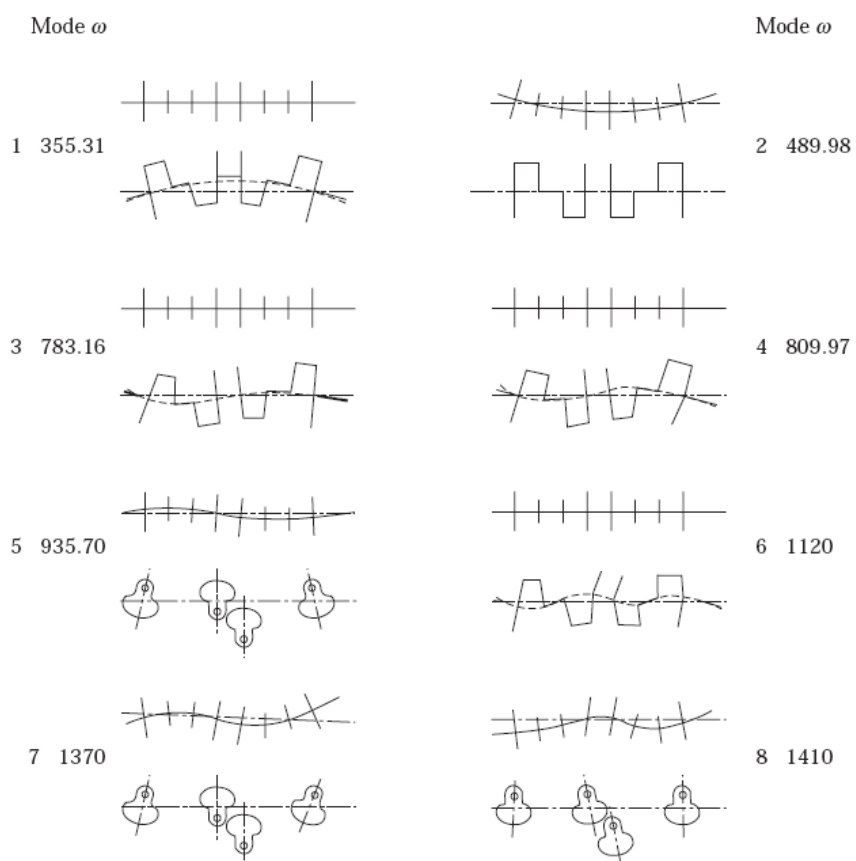


Figure 2.8: Mode shapes and frequency of a four cylinder crankshaft

Source: Kang, et al., 1997

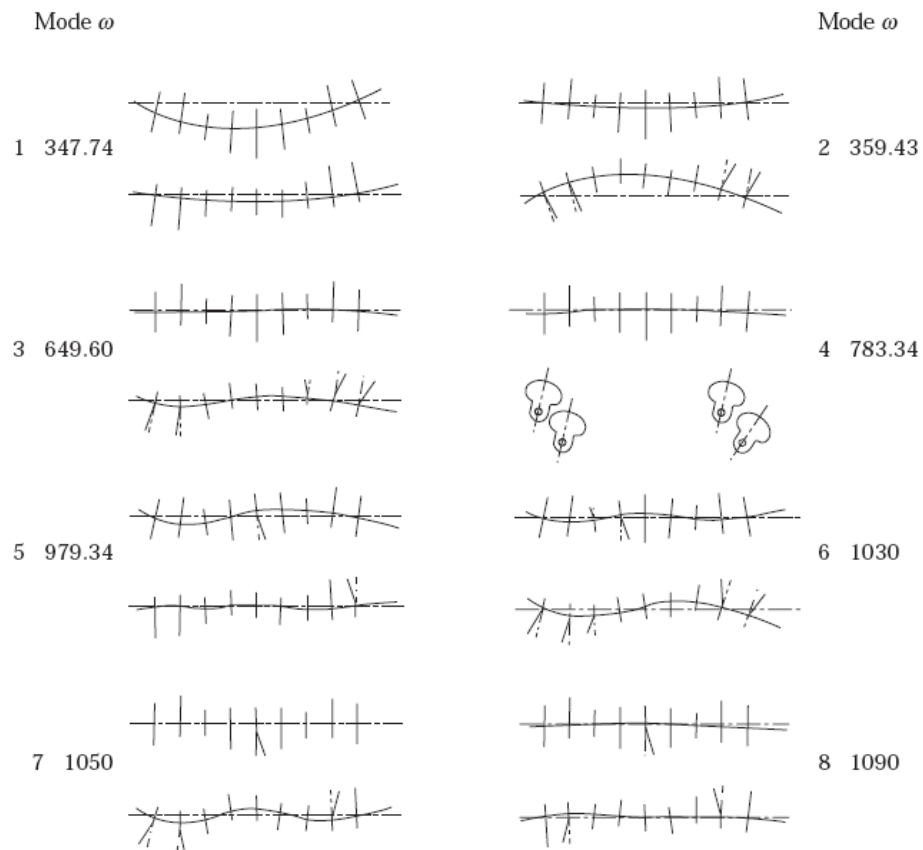


Figure 2.9: Mode shapes and frequency of a six cylinder crankshaft

Source: Kang, et al., 1997

2.5.2 A Crankshaft System Model for Structural Dynamic Analysis of Internal Combustion Engines

Although many researcher done in this field, Zissimos P. Mourelatos (2001) continues in analyzing the dynamic behavior of an internal combustion engine crankshaft is described. The model couples the crankshaft structural dynamics, the main bearing hydrodynamic lubrication and the engine block stiffness using a system approach. A two-level dynamic sub structuring uses a set of load. The main bearing lubrication analysis is based on the solution of the Reynold's equation.

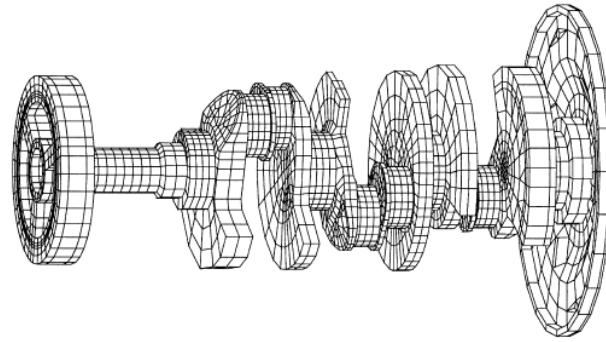


Figure 2.10: The finite element mesh for the pulley, crankshaft, flex plate system the PV6 engine

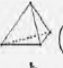




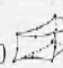
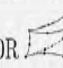
Source: Zissimos P. Mourelatos computer and structures (2001)

2.5.3 The Influence Of Finite Element Meshes On The Results Of A Spatial Polycrystalline Aggregate Model

The research by Igor Simonovskia, et al., (2010) clearly defined the influence of the micro structural inhomogenities in materials on the life-time of safety significant components of nuclear power plants is still not fully characterized. One of the most important sources of inhomogenities in metals is their grain structure. Differences in crystallographic orientations of grains lead to different responses under the applied loads and increased stresses at the grain boundaries. Engineering tools which are used to assess a response of a structural component to the applied loads are typically based upon the mechanics of continuum and are not able to account for these effects. Dedicated polycrystalline aggregate models are therefore being developed to study the effects of the microstructure on the load carrying capabilities of materials. However, a limited number of finite element types can be used due to the geometrical complexity of such models. A procedure for testing the behavior of different finite elements in simulations involving explicit models of randomly shaped and oriented grains described by crystalline elasticity and crystal plasticity is therefore proposed. Cumulative distributions of the stress/strain tensors in all integration points in the model are compared, enabling comparison of the “average” (macroscopic) as well as “extreme” (local) behavior of different meshes.

Such an approach provides an easy to use probabilistic measure of the quality of results obtained using different element types, formulations and mesh densities.

Table 2.1: The number of elements in the model.

ABAQUS el. type (no. nodes, no. int. points)	Average element size [μm]				Average element size [μm]			
	20.0	10.0	5.0	3.5	20.0	10.0	5.0	3.5
	Total number of elements				Elements per grain (average)			
C3D4  (4, 1)	11,371	52,542	417,486	1,137,609	53.6	247.8	1969.3	5366.1
C3D10  (10, 4)	11,371	52,542	417,486	1,137,609	53.6	247.8	1969.3	5366.1
C3D6  (6, 2)	3482	13,345	107,388	330,213	16.4	62.9	506.5	1558.6
C3D15  (15, 9)	3482	13,345	107,388	330,213	16.4	62.9	506.5	1558.6
C3D8  (8, 8)	3968	11,878	42,754	127,614	11.7	56.0	201.6	601.9
C3D20  (20, 27)	3968	11,878	42,754	127,614	11.7	56.0	201.6	601.9
C3D20R  (20, 8)	3968	11,878	42,754	127,614	11.7	56.0	201.6	601.9

Source: Igor Simonovskia, et al., 2010

CHAPTER 3

METHODOLOGY

3.1 INTRODUCTION

This chapter will mostly describe all the procedures used before, during and after both experimental and simulation method. For experimental method, PulseLab software was used to determine and capture all the signals detected by the sensors to determine the natural frequency. Solidworks and Algor software was used for simulation methods. Solidworks were used mostly to develop the crankshaft model in CAD and then Algor was used to simulate and analyse the crankshaft modal analysis and mode shapes. In simulations, precautions for mesh were generated and the locations of boundary conditions were taken into absolute consideration to obtain accurate results.

3.2 PROJECT FLOW CHART

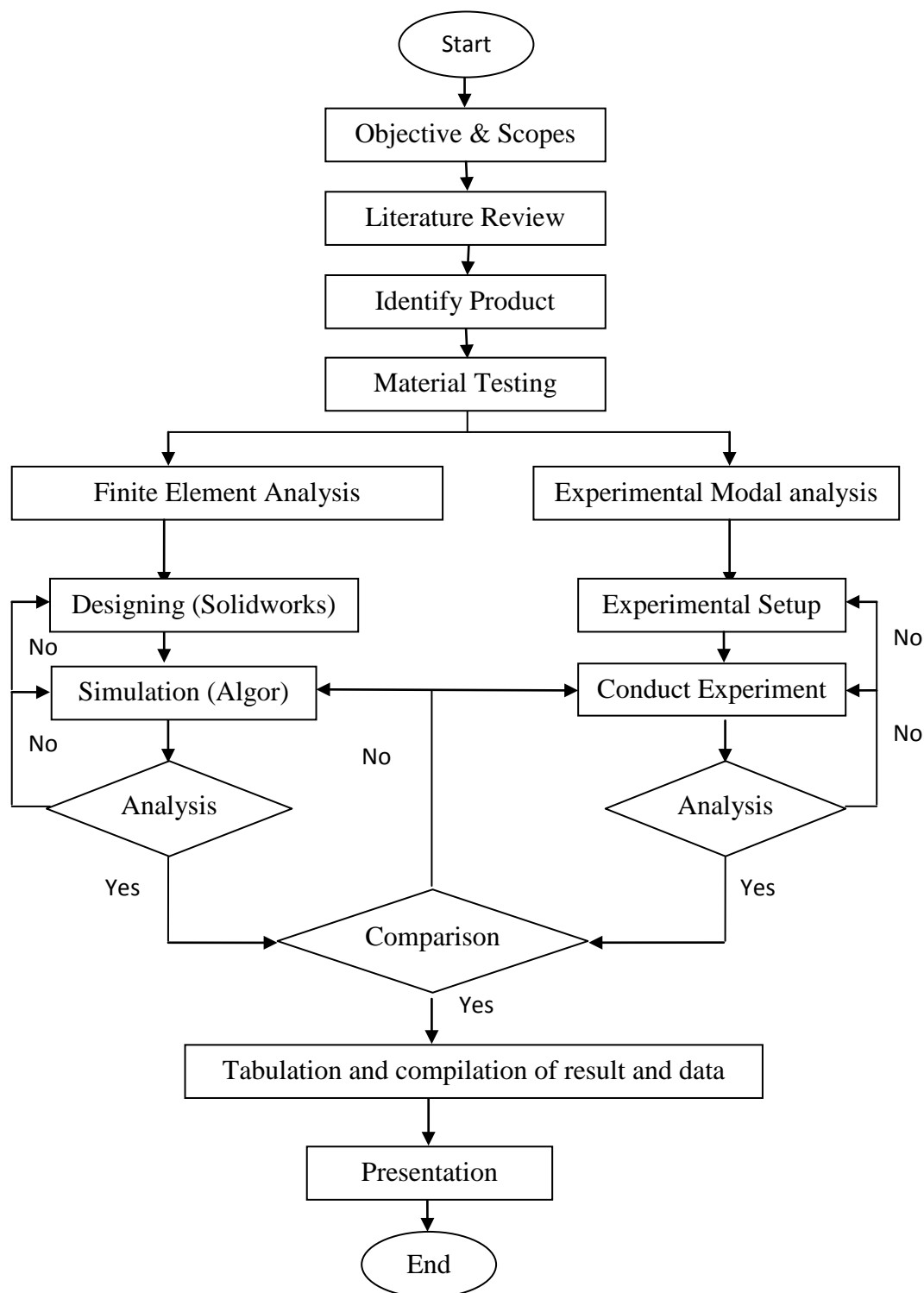


Figure 3.1: Project flow chart

3.2.1 Process Flow Description

In order to finish this project at the given time, flow chart as in Figure 3.1 was used as guidelines. This project was started by receiving the title of the project and by defining the objectives and scopes of this project. It was used as a guide for this project. After specifying the objectives and scopes, the literature review was done. The literature review part was completed by reviewing journals, books, doing research on the internet, and other related resources. In this part, data researched by other researchers were gathered and were used as a guidance and additional information. Later on, it was preceded with the methodology of this project in which the methods and the ways to conduct this project were delivered. After that, the project was continued by identifying the parts that we want to use for this project. Besides that, the material used to manufacture this part was identified by doing material test for this experiment. Identifying the material is important because the material's properties will be used to do analysis using the Algor Fempro software.

Firstly the projects were analysed using software. At the same time, the project were also analysed through experimental method. After that, both the analysed results were collected and comparisons were made. If the difference error is high, either the simulation or the experimental results must be checked for errors and the procedures are repeated. The error will be checked and the procedures will be repeated either from the beginning of designing process or the analysis. After the simulation have been completed , an experimental data were continued to be compiled into chapters which includes the introduction, literature review, methodology, analysis, discussion and conclusion following the format that had been given by the faculty. Finally, slides were prepared for presentation.

3.3 MATERIAL TESTING

The main purpose of material testing is to identify the compositions of the material inside the part that was used in this project. The Spectro Meter was used to conduct this experiment.



Figure 3.2: Spectro Meter

3.3.1 Determination of Material Composition

In order to conduct this process or experiment, several steps were followed in order to obtain an accurate result.

First of all, a flat surface at the crankshaft was found. The flat surface on crankshaft was grinded using 'Surface Grinder' to get an evenly flat surface. An evenly flat surface is important to obtain the accurate result. Then, polishing machine was used to polish the flat surface of the crankshaft.

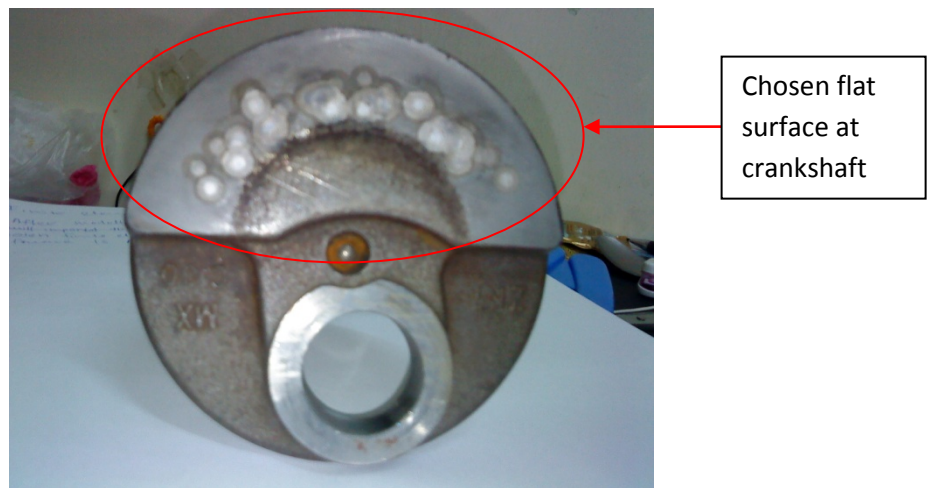


Figure 3.3: Chosen flat surface



Figure 3.4: Polishing machine

After that, Spectro Meter machine was used to find the compositions of the material. The proper type of testing was chosen. The same experiment was conducted several times to collect a series of result until the accurate composition of material was found.

Then data of the material's compositions were used to identify the type of material.

Table 3.1: Composition material of crankshaft

No.	Component Element	Testing (%)			Average (%)
		1	2	3	
1	Iron, Fe	96.6	96.7	96.7	96.7
2	Carbon, C	0.869	0.805	0.751	0.783
3	Silicon, Si	0.284	0.265	0.271	0.276
4	Manganese, Mn	0.913	0.927	0.939	0.926
5	Phosphorous, P	0.0169	0.0181	0.0182	0.0173
6	Sulfur, S	0.0030	0.0040	0.0033	0.0037
7	Chromium, Cr	1.05	1.05	1.04	1.05
8	Molybdenum, Mo	0.0050	0.0057	0.0050	0.0050
9	Nickel, Ni	0.0335	0.0322	0.0360	0.0366
10	Aluminum, Al	0.0394	0.0327	0.0331	0.0342
11	Cobalt, Co	0.0073	0.0080	0.0080	0.0078
12	Copper, Cu	0.0317	0.0317	0.0326	0.0325
13	Niobium, Nb	0.002	0.002	0.002	0.002
14	Titanium, Ti	0.0888	0.0814	0.0827	0.0853
15	Vandium, V	0.002	0.002	0.002	0.002
16	Tungsten, W	0.0150	0.0150	0.0150	0.0150
17	Lead, Pb	0.0250	0.0250	0.0250	0.0250

The Table 3.1 shows the compositions of material of the crankshaft, which were obtained from the Spectro Meter machine. There were seventeen elements in the crankshaft. From the seventeen elements found, the major elements were Iron (Fe), Chromium (Cr), Carbon (C) and Manganese (Mn).

3.3.2 Identifying the Material of the Crankshaft

The type of material was identified by using material composition data as shown in Table 3.1. In order to do this, two books were used as the main reference to identify the type of material. The books used were, Engineering Material 1 and Engineering Material 2 written by Michael Ashby and DRH Joney.

This book gave a broad introduction about the properties of material used in engineering application. It also provided a complete introductory course in engineering material for students with no previous background in this subject.

Although the type of material was completely identified by using books, there were also some online links to identify the type of material using material's properties data. It was easier compared to reference from the two books.

The material for this crankshaft is High Carbon Steel and the material's properties are shown in Table 3.2.

Table 3.2: Material Properties

Physical Properties	Metric	English
Density	0.451 - 8.26 g/cc	0.0163 - 0.298 lb/in ³
Particle Size	6.70 - 12.0 μm	6.70 - 12.0 μm
Chemical Properties		
Critical Temperature	168 - 1550 °C	334 - 2830 °F
Mechanical Properties		
Hardness, Brinell	170 - 600	170 - 600
Hardness, Knoop	195 - 875	195 - 875
Hardness, Rockwell B	43.0 - 100	43.0 - 100
Hardness, Rockwell C	10.0 - 70.0	10.0 - 70.0
Hardness, Vickers	182 - 848	182 - 848
Tensile Strength, Ultimate	161 - 3200 MPa	23300 - 464000 psi
Tensile Strength, Yield	275 - 2750 MPa	39900 - 399000 psi
Elongation at Break	0.500 - 30.0 %	0.500 - 30.0 %
Reduction of Area	13.4 - 73.0 %	13.4 - 73.0 %
Rupture Strength	621 - 1300 MPa	90000 - 189000 psi
Modulus of Elasticity	13.8 - 235 GPa	2000 - 34100 ksi
Flexural Yield Strength	159 - 5130 MPa	23000 - 744000 psi
Compressive Yield Strength	1320 - 3100 MPa	191000 - 450000 psi
Bulk Modulus	140 GPa	20300 ksi
Poissons Ratio	0.280 - 0.313	0.280 - 0.313
Charpy Impact	1.36 - 99.0 J	1.00 - 73.0 ft-lb
Charpy Impact, Unnotched	2.71 - 86.0 J	2.00 - 63.4 ft-lb
Izod Impact	3.00 - 18.0 J	2.21 - 13.3 ft-lb
Izod Impact Unnotched	10.8 - 229 J	8.00 - 169 ft-lb
Machinability	10.0 - 125 %	10.0 - 125 %
Shear Modulus	64.1 - 81.7 GPa	9300 - 11900 ksi
Abrasion	8.00 - 85.9	8.00 - 85.9

3.4 DEVELOPING AND MODELLING THE CRANKSHAFT

In order to perform the simulation analysis, the crankshaft was developed by using CAD programme. The CAD programme that was used to develop and draw the 3D model of the crankshaft is Solidworks 2010.

The dimension of crankshaft to be modelled in CAD program was taken directly from the real part. The dimension was taken as accurate as possible to assure that the result from simulation correlates with experimental data.

The crankshaft modelling was carried out part by part. After doing so, the part is assembled together one by one before saving the work in IGES format.

During the modelling, there was some simplification on drawing, in which the modelling of the crankshaft was done without any fillet in drawing. This was done to avoid errors occurring during simulation using Algor software.

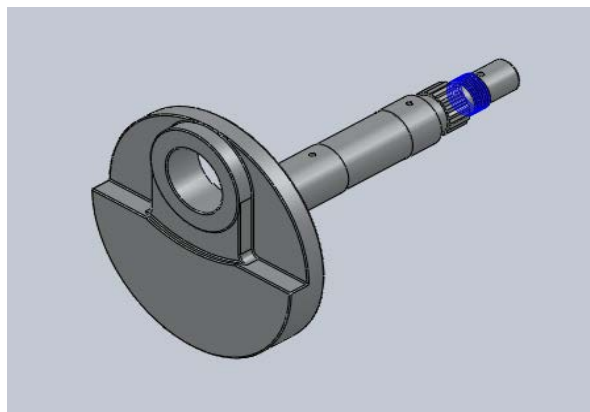


Figure 3.5: First part modelling in Solidworks 2010

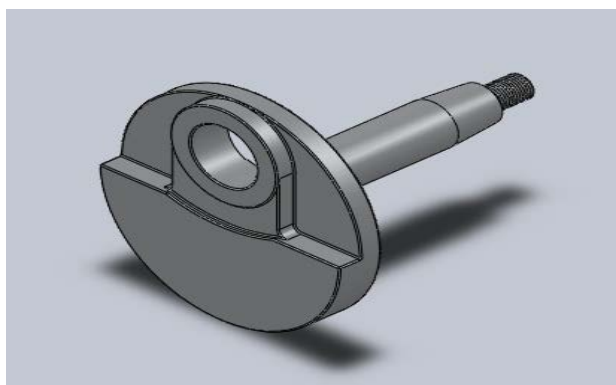


Figure 3.6: Second part modelling in Solidworks 2010

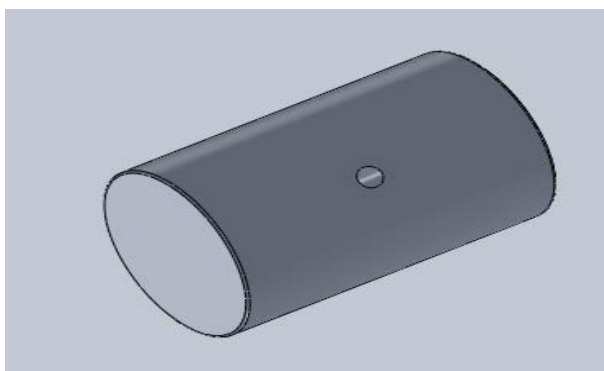


Figure 3.7: Third part modelling in Solidworks 2010

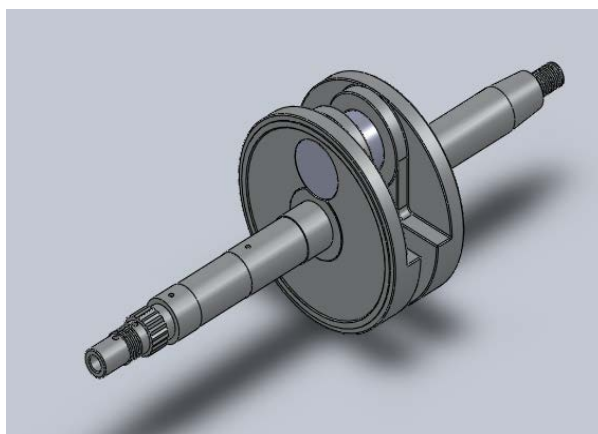


Figure 3.8: Completed crankshaft assembly

3.5 FINITE ELEMENT ANALYSIS

After modelling the crankshaft using Solidworks software, it was imported to choose Finite Element Analysis software. All the files in Solidworks needed to be saved in 'IGES' format. For this project, the chosen software was Algor Fempro 23.1 to further analyse the crankshaft modal analysis and mode shapes. At the same time, selection of Analysis type, Element type, Element definition and Material Properties must be done carefully. More consideration needs to be taken into account especially on mesh density, as a coarse mesh will generally give poor results. Tetrahedrons were used as the element type. All the material's properties such as modulus elasticity, mass density, and Poisson's ratio, thermal coefficient of expansion and shear modulus of elasticity were obtained from the experimental of material testing. Then the modelled crankshaft needs to mesh with the suitable mesh ratio. All the data generated by Algor were recorded and stored for further comparison.

3.5.1 Analysis Type

First of all, the analysis type was chosen before starting the simulation using Algor. The analysis type depends on which type of analysis will be conducted.

In this research, the chosen analysis type was 'Natural Frequency' (modal) according to the research title. This analysis type will be able to calculate the natural frequency and the mode shapes.

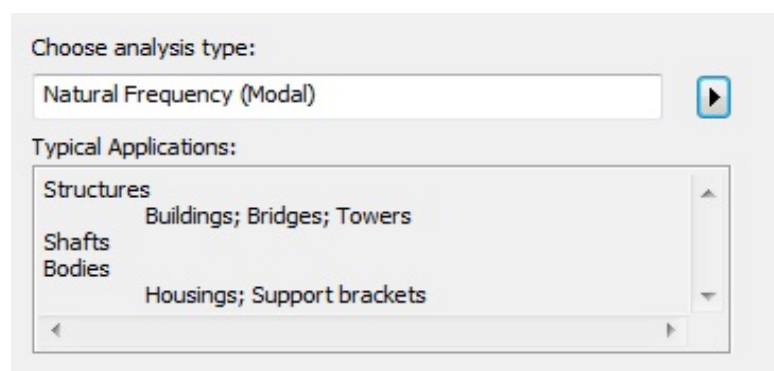


Figure 3.9: Chosen analysis type in Algor software

3.5.2 Element Type

In FEA software choosing element type is an important parameter. Algor software has several types of element types. Those are:-

1. All Bricks
2. All Tetrahedra
3. Bricks and Tetrahedra
4. Tetrahedra and Wedges
5. Bricks and Wedges

Each element types have their own function when doing the simulation.

In order to do the simulation, Tetrahedra was chosen as an element type. This is because, (Xavier BOURDIN, 2002) and (Miomir Jovanovic, 2010) stated in research that the tetrahedral element stability was found to be excellent. For more complex shapes, the increased computing cost may be largely outweighed by the advantages of an automatic meshing approach.

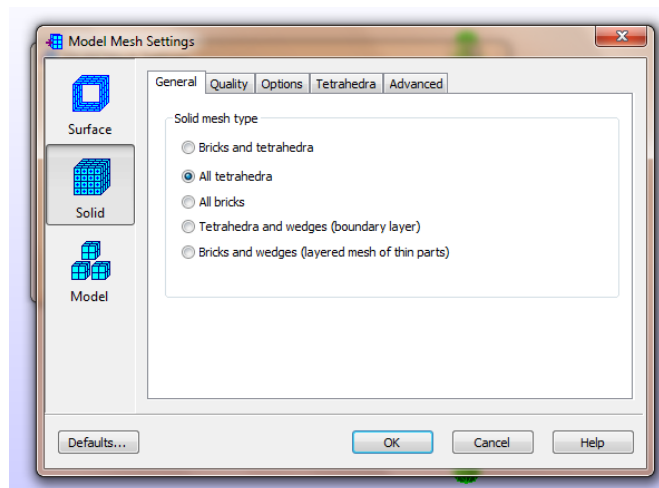


Figure 3.10: Model mesh setting

(Y. Kang, 1997) stated that if an engine crankshaft is modelled by beam element, the result of analysis is somewhat questionable compared to a solid modelled. Since the crankshaft was modelled in Solidworks with fine accuracy, Algor FEMPRO will mesh the modelled with solid element.

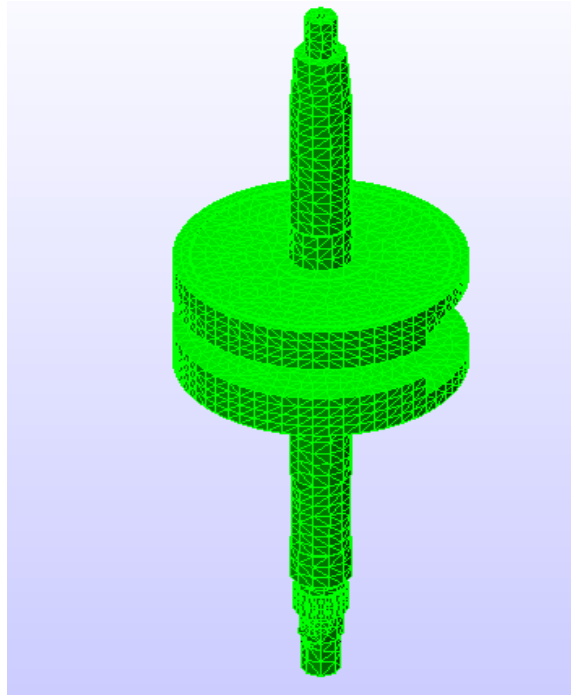


Figure 3.11: Model after complete meshing

3.5.3 Material Properties

Material properties are very important parameters in Algor software. To conduct analysis, the types of materials should be chosen similar to actual model of crankshaft. This will give an accurate result when doing simulation.

When filling the data in table, element material specification must be in proper units. The units must be the same as a crankshaft modelling in Solidworks software.

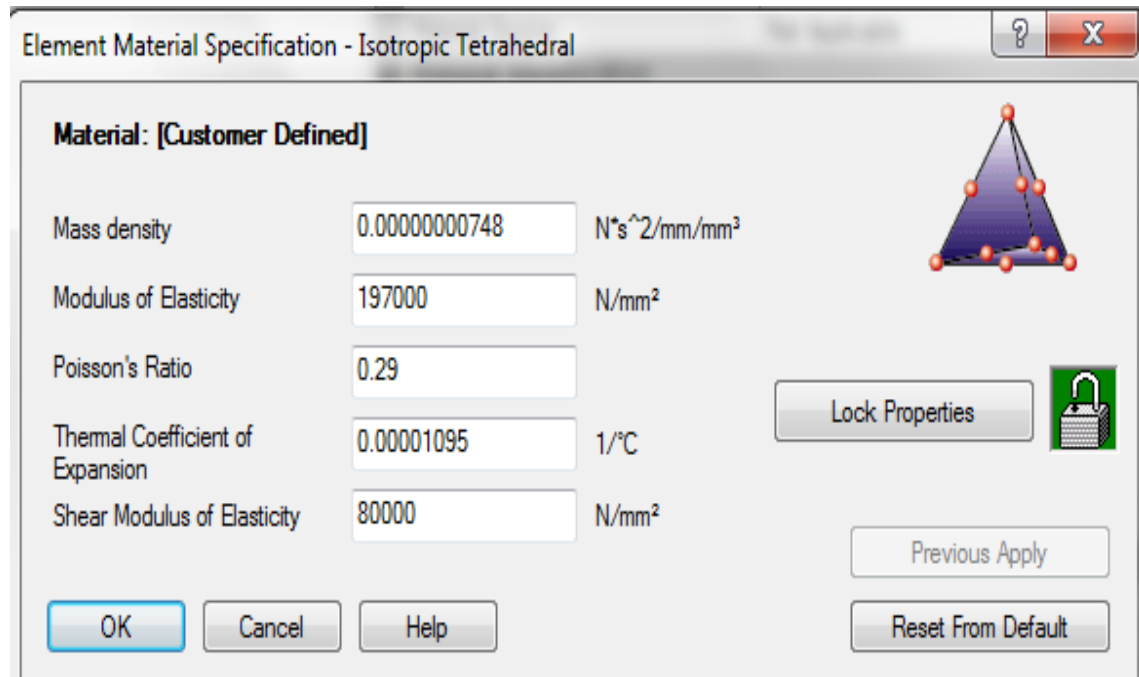


Figure 3. 12: Element material specification

3.6 EXPERIMENTAL MODAL ANALYSIS

In experiment, a crankshaft, a test rig and a sensor are needed. Data acquisition system (DAS) was also used in order to obtain the result from the sensors. The DAS used for this experiment test was 8 channels FFT Analyzer with PulseLab software.

3.6.1 Introduction about Pulse

PULSE™ is Brüel & Kjær's platform for noise and vibration analysis and has of over a 60 years of measurement experience and innovation.

Developed as an advanced solution for sound and vibration measurement, PULSE™ is the analyzer platform of the future. With its vast range of software applications and hardware configurations PULSE is today probably the most popular analyzer solution in the world with over 10.000 systems sold.

The PULSE hardware or software family is a solid foundation upon which to build a system to suit present needs, and which can also be extended as requirements change from time to time. This expandability, and the continuing development of new PULSE applications and hardware, ensures the safety in the present and in the future.

3.6.2 List of Apparatus

Below are the list of apparatus used for this experiment and simulation.

Table 3.1: List of apparatus

No	Apparatus	Function
1	8 Channel FFT Analyzer Model: PULSE Type 3560 C	Used to collect time data and convert it to the FRF measurement. Then, responses will be displayed in the computer.
2	Computer with PULSE-Lite software version 11.1, Solidworks 2008 and Algor FemPro V21	PULSE-Lite is used to display the collected data. Solidworks is used to create a CAD modeled of the crankshaft and Algor is used in simulation for modal analysis.
3	Accelerometer Model: Bruel & Kjaer Type 4507-B	Used to measure the response signal from each DOF from impact hammer test.
4	Impact Hammer Model: ENDEVCO Type 2302-10	Used to impact all the DOF's point on the crankshaft. The tip on the impact hammer is plastic.



Figure 3.13: Impact hammer used in experiment



Figure 3.14: The data acquisition system



Figure 3.15: Single-Axial accelerometer

3.6.3 Experiment Setup

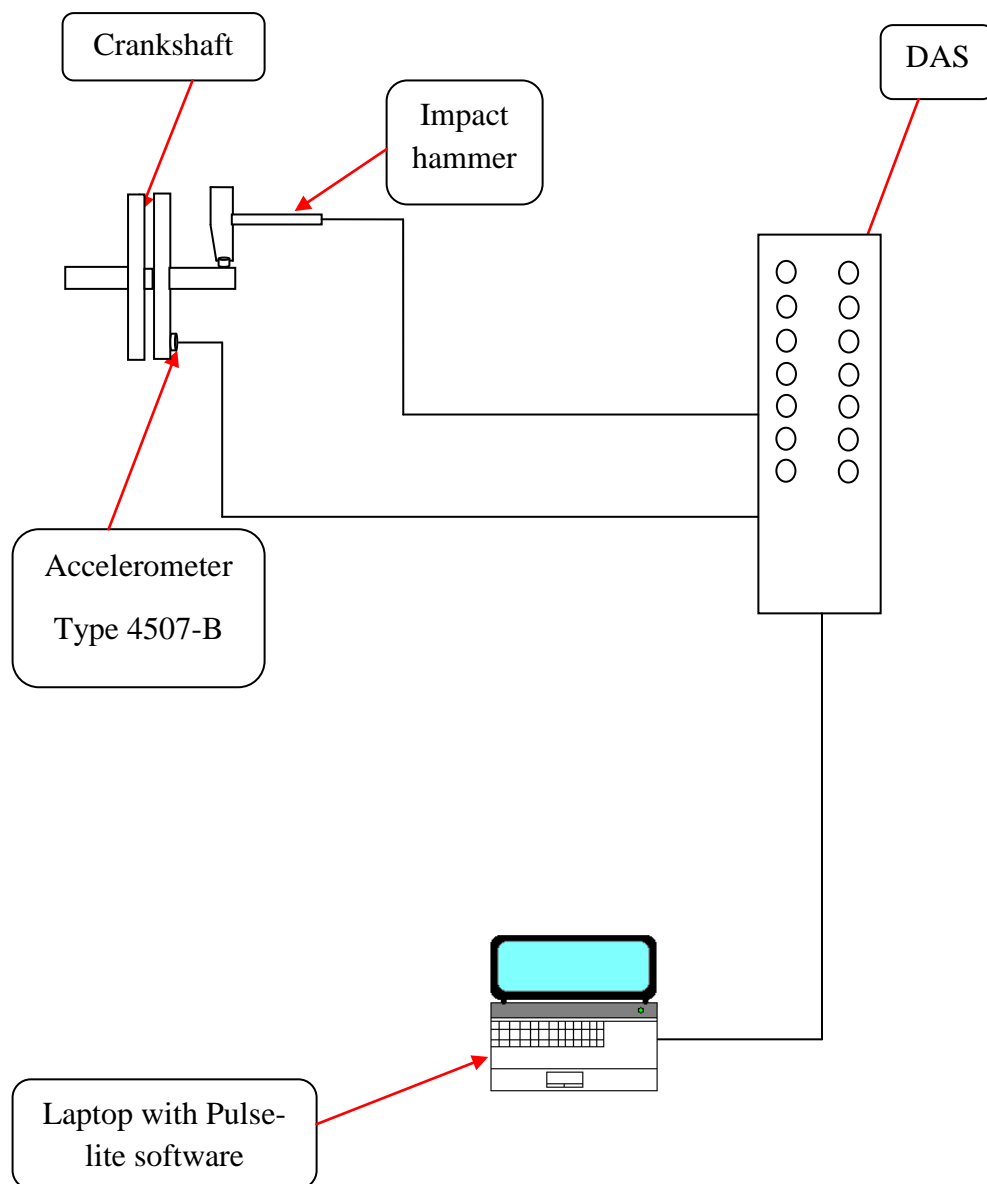


Figure 3.16: Impact hammer testing setup

The crankshaft was mounted on the table and covered by sponge in order to achieve free boundary condition. The Single-axial accelerometer sensor, which sense any signal or input mounted on the crankshaft at a designated place. The crankshaft was hit using an impact hammer at nine different points. The vibration that occurred after the impact was recorded using data acquisition system with Pulselab software. Data from Pulselab was compiled and then was exported for further analysis. From here, the signal taken from the sensor was calculated and the natural frequency from mode one until mode five was determined.

CHAPTER 4

RESULT AND DISCUSSION

4.1 INTRODUCTION

This chapter will show the result of all the analysis carried out. The result for this analysis was obtained through simulation using the Algor software and experimental using impact hammer test. Besides that, comparison between simulation and experiment methods of modal analysis is displayed and discussed.

4.2 FINITE ELEMENT MODEL

Figure 4.1 until 4.6 shows Finite Element Model developed in ALGOR. The complete model shows model geometry, mesh design and Boundary Condition.

Using the Finite Element Model, simulation of Modal Analysis for maximum five modes were carried out. Figure 4.1 until 4.6 shows first simulated frequency value with associated mode shapes which are displayed in Table 4.1. Other simulation results are shown in appendix. The Table 4.2 shows overall result with different mesh size.

4.2.1 First Simulation

Mesh Aspect Ratio : 100%
Final Mesh Size : 4.74031
Total Element Create : 6750
Element type : Tetrahedron

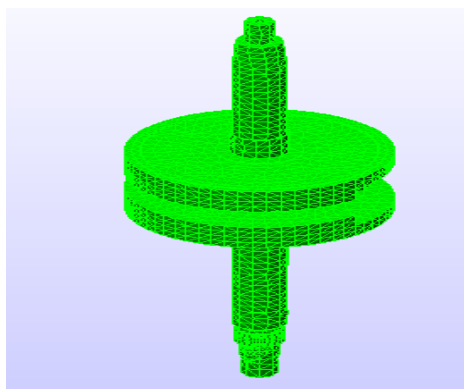


Figure 4.1: Mesh Model for First Simulation

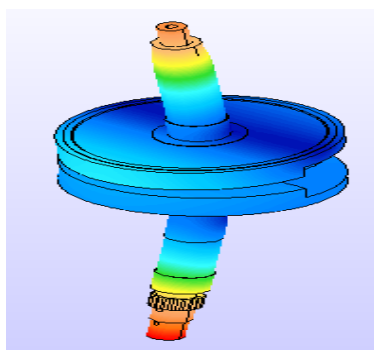


Figure 4.2: Mode shape 1

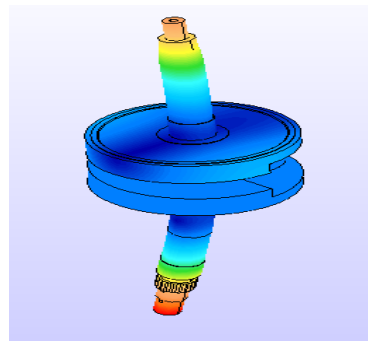


Figure 4.3: Mode shape 2

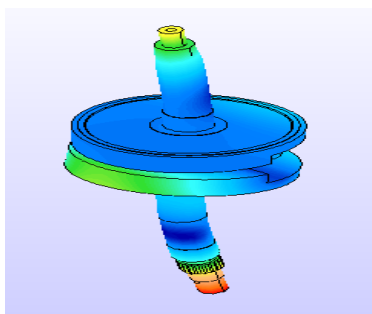


Figure 4.4: Mode shape 3

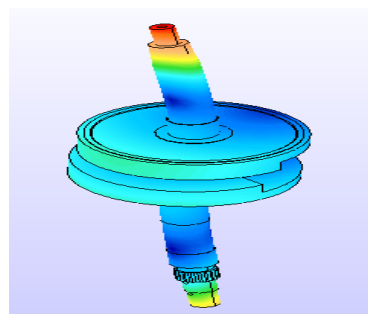


Figure 4.5: Mode shape 4

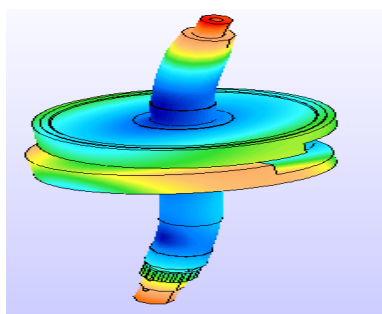


Figure 4.6: Mode shape 5

Table 4.1: Frequency of First Simulation

Mode Shape	Frequency (Hz)	Deflection Type
1	1160.12	Bending In face off
2	1310.58	Bending In face axis
3	2256.25	Bending out of face
4	2328.43	Bending out of face
5	2797.93	Bending out of face

Table 4.2: Mode Shape and Frequency in Different Mesh Aspect Ratio

Mode Shape	100%	90%	80%	70%	60%
1	1160.12	1128.73	1106.17	1086	1059.6
2	1310.58	1276	1252.73	1231.99	1204.59
3	2256.25	2207	2174.52	2144.12	2104.59
4	2328.43	2288.33	2245.92	2217.83	2174.66
5	2797.93	2754.11	2705.7	2674.34	2624.24

4.3 SIMULATION RESULT

Finite Element Analysis was carried out by using Algor software to determine natural frequency and mode shape. Five different mesh ratios were used to carry out the simulation. These different mesh ratios give a more accurate result which is similar to the experiment.

Each different mesh size gave different final mesh size and natural frequency. Table 4.2 shows the element of mesh used and the final mesh.

Table 4.3: Element Type and Final Mesh Ratio

Mesh Aspect Ratio	Element Type	Final Mesh Size
100 %	Tetrahedron	4.74031 mm
90 %	Tetrahedron	3.94637 mm
80 %	Tetrahedron	3.22341 mm
70 %	Tetrahedron	2.57162 mm
60 %	Tetrahedron	1.48135 mm

4.4 INFLUENCE OF ELEMENT OR MESH TYPE

Mesh study was performed on the FE model to ensure sufficiently fine sizes are employed for accuracy of the calculated result depending on the CPU time. During the analysis, the specific variable and the mesh convergence was monitored and evaluated. The mesh convergence is based on the geometry, model topology and analysis objectives.

(Xavier BOURDIN, 2002) stated that the finite element tetrahedron is the most frequently used in automatic procedures of modern software for the discrete continuum modeling. Tetrahedron is characterized by four nodes among which the movements of the continuum are interpolated by functions of form. Such as, small number of nodes in relation to the brick (the eight-node element) or other more complex elements has varying success in describing the internal stress-strain state of structures. The reason for the application of tetrahedron lies in the ease of description of the complex topology of structures and the working speed of grid generator.

Furthermore, (Miomir Jovanovic, 2010) also stated in research the tetrahedral element stability was found to be excellent. For more complex shapes, the increased computing cost may be largely outweighed by the advantages of an automatic meshing approach.

4.5 EXPERIMENTAL RESULTS

The experimental result was taken from the FRF data in PulseLab software. Figure at Appendix B shows the frequency on each point measured during experiments. The data on nine points were measured to obtain the graph to identify the natural frequency.

4.6 GRID – POINT NATURAL FREQUENCY

Figure 4.7 shows Frequency Response Function (FRF) developed in PLUSELAB software.

The frequency response function of the SDoF system can be displayed in a number of different ways. Each display method is able to highlight a specific aspect of FRF. Through different ways of FRF display, some interesting properties of the FRF were revealed.

Using the FRF graph, the experimental of Modal Analysis for maximum five modes carried out were obtained. Figure 4.7 shows experimental frequency value associated with Damping ratio are displayed in Table 4.4. Other experiment results are shown in appendix. The overall experiment result is shown in Table 4.5 according to different point.

4.6.1 First Point

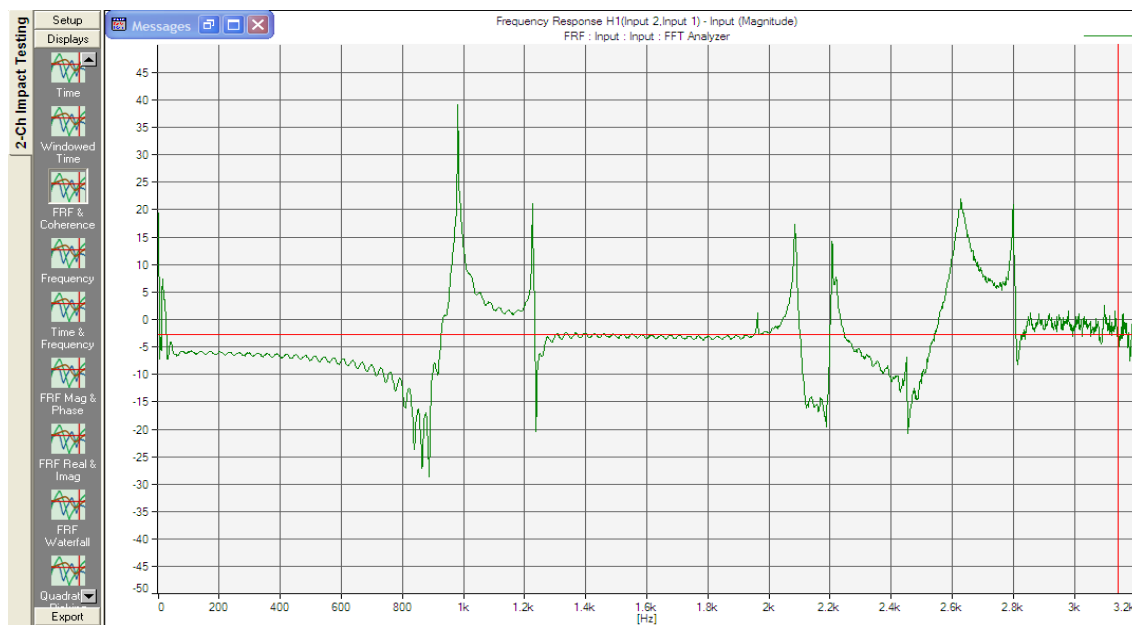


Figure 4.7: Frequency Measured At Point 1

Table 4.4: Value of Natural Frequency in Different Mode Shape at Point 1

Mode Shape	Frequency (Hz)	Damping ratio
1	990	0.09
2	1224	0.109
3	2084	0.094
4	2204	0.343
5	2798	0.069

Table 4.5: Result of Experimental Modal Analysis (Impact Hammer Test)

Mode	1	2	3	4	5
Shapes					
Point	(Hz)	(Hz)	(Hz)	(Hz)	(Hz)
1	990	1224	2084	2204	2798
2	990	1224	2084	2218	2798
3	990	1224	2084	2218	2798
4	990	1222	2086	2224	2782
5	990.12	1224	2082	2216	2798
6	990	1226	2086	2222	2800
7	990	1226	2086	2222	2800
8	990	1220	2086	2224	2776
9	990	1226	2086	2224	2776

Table 4.6: Average Result of Experimental Modal Analysis (Impact Hammer Test)

Mode Shape	Natural Frequency (Hz)
1	990.01
2	1224
3	2084.89
4	2219.11
5	2791.18

4.7 COHERENCE FUNCTION

The coherence function describes the linear and casual links between one output signal and all known input signals. It can be used to evaluate the influence of unknown inputs to an output. These unknown inputs may be measurement noise, energy leakage or nonlinearity. Every output has a multiple coherence. If it equal to one, the output is correlated with all inputs. If it is equal to zero, the output is due to unknown inputs such as noise.

Figure 4.8 and 4.9 shows the relationship between FRF and Coherence

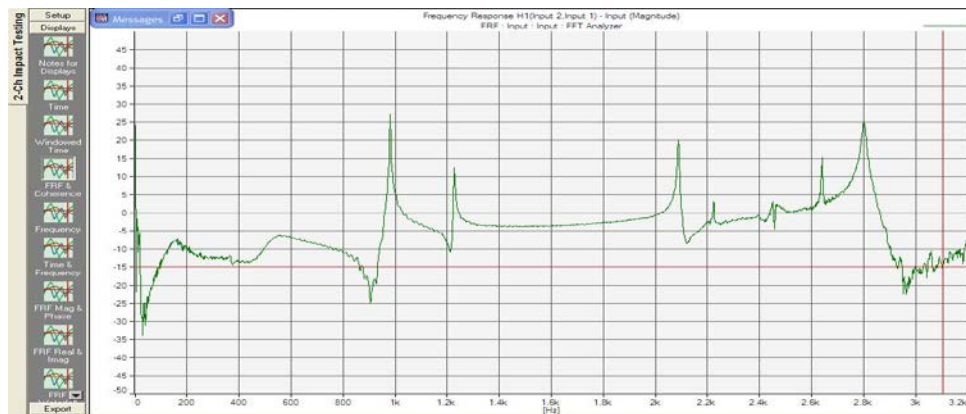


Figure 4.8: FRF at Point 6

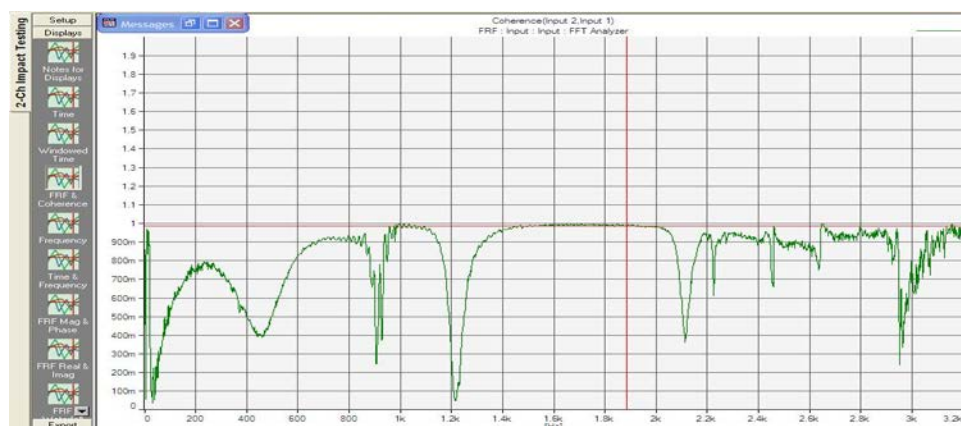


Figure 4.9: Coherence at Point 6

4.8 COMPARISON OF EXPERIMENTAL AND SIMULATION

In this section, the natural frequency on each mode shapes is compared between experimental and simulations. Detailed comparison including errors calculated is shown in Table 4.7 until 4.11 in their respective mode shapes and mesh aspect ratio.

From the comparison that shown at Table 4.7 until 4.11 clearly shows, the smaller mesh size will give the smallest error between simulation and experiment results.

Table 4.7: Comparison On Experimental and Simulation Data, Mode Shapes From Experiment with Mode Shapes from Simulation At 100% Aspect Mesh Ratio

Mode Shapes	Experimental Natural Frequency, Hz	Simulation Natural Frequency, Hz	Error (%)
1	990.01	1160.12	14.66
2	1224	1310.58	6.61
3	2084.89	2256.25	7.59
4	2219.11	2328.43	4.70
5	2791.18	2797.93	0.24

Table 4.8: Comparison On Experimental and Simulation Data, Mode Shapes From Experiment with Mode Shapes from Simulation At 90% Aspect Mesh Ratio

Mode Shapes	Experimental Natural Frequency, Hz	Simulation Natural Frequency, Hz	Error (%)
1	990.01	1128.73	12.29
2	1224	1276	4.08
3	2084.89	2207	5.53
4	2219.11	2288.33	3.02
5	2791.18	2754.11	1.35

Table 4.9: Comparison On Experimental and Simulation Data, Mode Shapes From Experiment with Mode Shapes from Simulation At 80% Aspect Mesh Ratio

Mode Shapes	Experimental Natural Frequency, Hz	Simulation Natural Frequency, Hz	Error (%)
1	990.01	1106.17	10.50
2	1224	1252.73	2.29
3	2084.89	2174.52	4.12
4	2219.11	2245.92	1.19
5	2791.18	2705.7	3.06

Table 4.10: Comparison On Experimental and Simulation Data, Mode Shapes From Experiment with Mode Shapes from Simulation At 70% Aspect Mesh Ratio

Mode Shapes	Experimental Natural Frequency, Hz	Simulation Natural Frequency, Hz	Error (%)
1	990.01	1086	8.84
2	1224	1231.99	0.65
3	2084.89	2144.12	2.76
4	2219.11	2217.83	0.06
5	2791.18	2674.34	6.98

Table 4.11: Comparison on Experimental and Simulation Data, Mode Shapes From Experiment With Mode Shapes From Simulation At 60% Aspect Mesh Ratio

Mode Shapes	Experimental Natural Frequency, Hz	Simulation Natural Frequency, Hz	Error (%)
1	990.01	1059.6	6.56
2	1224	1204.59	1.59
3	2084.89	2104.59	0.94
4	2219.11	2174.66	2.00
5	2791.18	2624.24	5.98

4.9 SUMMARY OF RESULT

4.9.1 Discussion on Graph of Natural Frequency versus Mesh Size

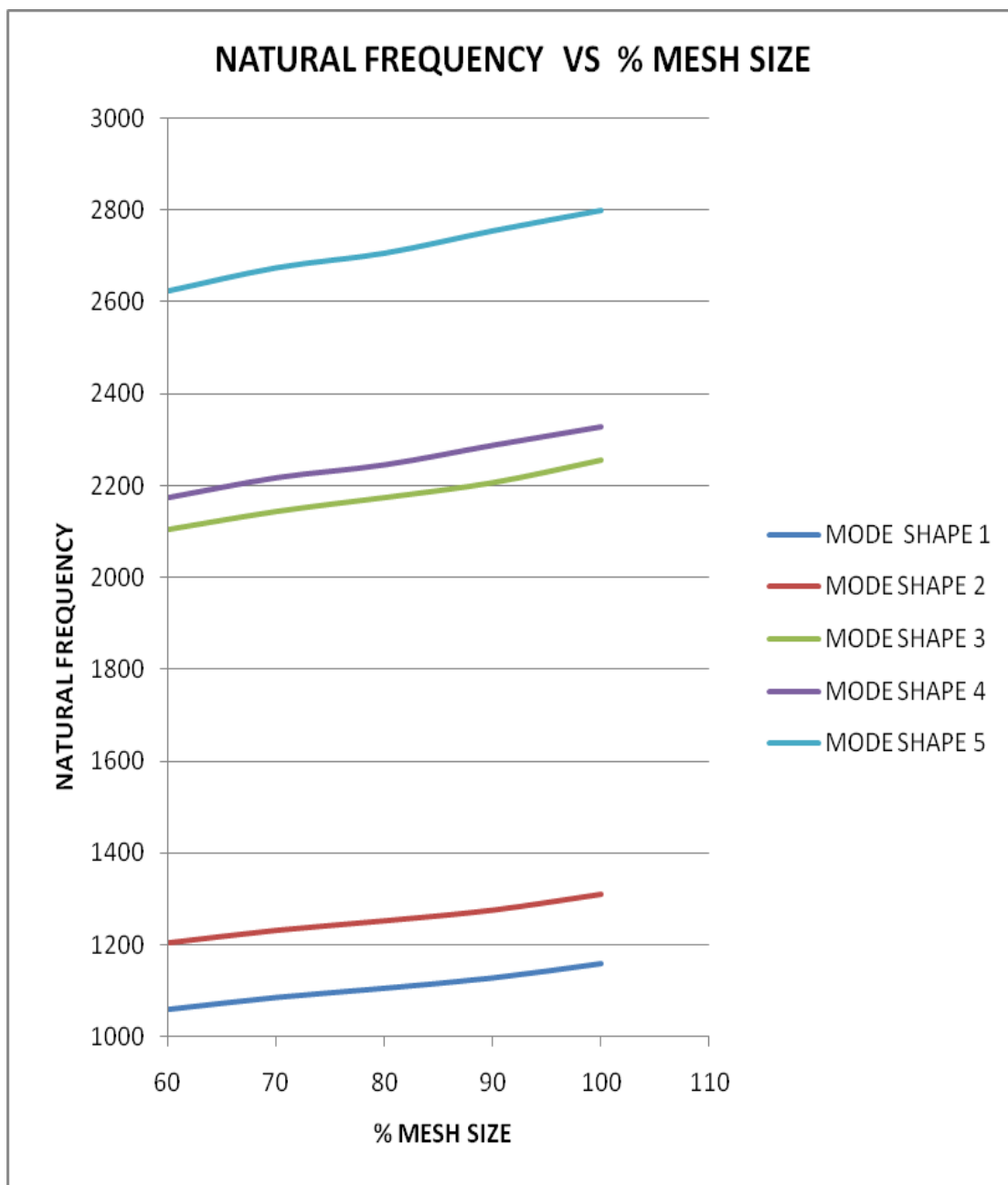


Figure 4.10: Graph of Natural Frequency vs. % mesh size

From the graph in Figure 4.10, it can be concluded that at all mode shapes of the natural frequency obtained in the analysis increases with the increase in percentage of mesh size. This is due to the reason that a decrease in mesh size will give a low natural frequency compared to large mesh size. When the percentage of mesh size is small, the analysis will be done in a more detailed manner as compared to when there are more meshes on the particular subject analysis. A more detailed analysis brings greater accuracy to the analysis, hence a lower natural frequency is obtained.

In simple words, smaller mesh will bring an accurate result for simulation.

4.9.2 Discussion on Graph of Mesh Size versus Mesh Aspect Ratio

The graph in Figure 4.11 shows the relationship between Mesh size and Mesh Aspect Ratio. The trend of graph clearly shows that the mesh size will decrease when mesh aspect ratio is reduced. When the mesh size is small, automatically the total element in the model of the crankshaft in Algor will increase. This will help to get a more accurate simulation result.

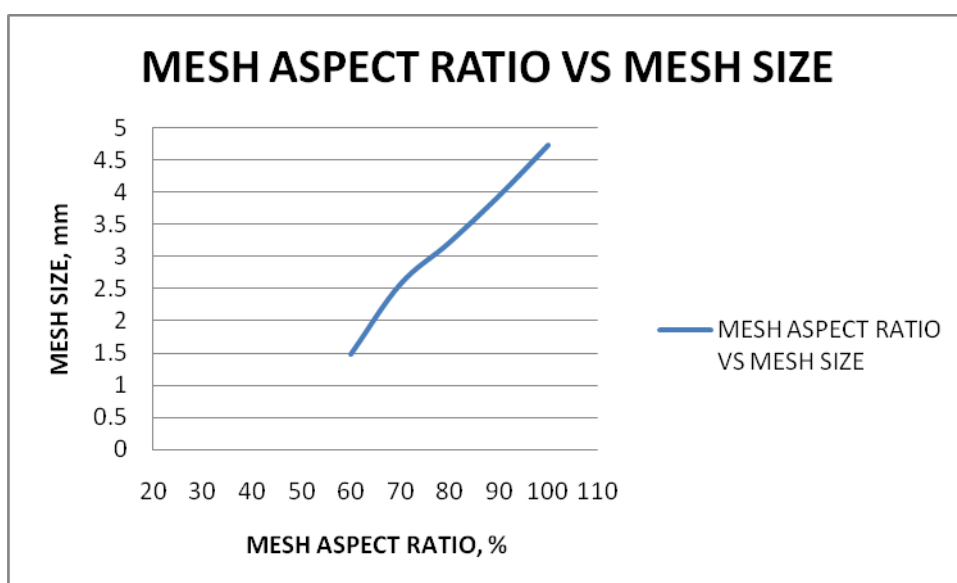


Figure 4.11: Graph of Mesh Size vs. Mesh Aspect Ratio.

4.9.3 Discussion on Comparison between Simulation and Experiment.

The Table 4.7 until 4.11 above show the comparisons of results between experimental and simulation at different aspect mesh ratio.

The result also shows that at 100 % mesh aspect, the error between experimental and simulation is in high value. Meanwhile at 60 % mesh aspect ratio, the error is very small compared to others mesh aspect ratio. This is because when using smaller mesh aspect ratio, the Algor software will generate more element and smaller final mesh size at the crankshaft model compared to high mesh aspect ratio.

According to Xavier BOURDIN [10] in the numerical science, when more elements exists in a model it will produce an accurate result of natural frequency.

From this, it can be concluded that the usage of smaller mesh aspect ratio gives a more accurate result while running the simulation in Algor.

4.10 OVERALL DISCUSSION

From Table 4.7 until 4.11, the comparison between simulation and experimental data different mesh aspect ratio are shown. The percentage of errors between these two data was calculated. Different mesh sizes generate different value of natural frequency, thus different percentage of errors were calculated from the data.

The experiment was run on some assumptions which are static working condition, and free boundary condition. Where else for simulation assumptions were free boundary condition, solid modeling, crankshaft model is accurate and near precise with the real crankshaft without any fillet and material chosen is same as the real crankshaft.

4.11 JUSTIFICATION FROM THE RESULT

From the results that have been obtained, it can be justified that for simulation, type of materials should be similar to actual model of crankshaft, boundary conditions must be determined, element material specification must be in the correct unit which is similar in the CAD modeling and finally a smaller mesh size must be used.

Whereas for the experimental results, a suitable modal analysis experiment must be chosen, PULSE LabShop software version 11.1-hammer 2_2 is chosen and degree of freedom (DOF) to vary result must be increased.

CHAPTER 5

CONCLUSION AND RECOMMENDATION

5.1 INTRODUCTION

In this chapter, the results of both experimental and simulation are summarized. Recommendations on future research for engine crankshaft are included further in this chapter.

5.2 SUMMARY

At the beginning of this project, crankshaft is modeled in Solidworks software. In this project, the real challenge is to model the crankshaft in Solidworks software for computer analysis. The crankshaft need to be modeled as precisely as possible since the result for both simulation and experiment will be compared. Even a single mistake in modeling can result in significance error margin when comparing the results. Then, when computer analysis is started, some assumptions need to be taken into consideration.

In the experiment, the real crankshaft is supported by a sponge to simulate free boundary conditions. Nine degree of freedoms (DOF) is selected as appropriate points for impact. Then the crankshaft is hit with an impact hammer at all the DOF. The data detected using the single-axial accelerometer is sent to the DAS to further analyse its frequency response. After both results for simulation and experimental have been obtained, comparison and analysing can be done.

5.3 CONCLUSIONS

Both experiment and simulation is performed to determine the crankshaft natural frequency and mode shapes. The errors calculated from Table 4.7 until 4.11 shows a lowest error margin in fine mesh but a higher error margin in coarse mesh. Since the lowest average error is in 60% mesh aspect ratio, the data will be used in the final simulation results.

Mode shape deflections (shown in Figure 4.1 until 4.6) vary from modes to modes. This mode shapes can possibly happen in the real life situation when the working frequencies of the crankshaft is equal to the natural frequency on each mode. For example, in the first mode, the deflection type is bending with the natural frequency at 1160.12/s with maximum deflection range at about 109.873 mm.

Thorough research on working frequency and natural frequency of the crankshaft is crucial to avoid resonance during operation.

5.4 RECOMMENDATIONS

Based on the result that has been analysed, several recommendations can be issued to make the result more reliable and reduce the percentage error of the analysis. The errors margin shown in Table 4.7 until 4.11 clearly shows the varied error. This is because, lots of assumption is considered. Below are some recommendation that can further reduce the errors between simulation and experimental.

For simulation, the result will be more accurate and errors can be lessened by using other CAE tools, such as PATRAN and Simulia ABAQUS. Besides that, using data from manufacturer such as modulus elasticity and density of material can further enhance the simulation analysis. Finally, the boundary conditions can be fixed during the simulation.

On the other hand, for the experiment, data from PulseLab software is obtained and then Me'scopeVes software is used to interpret data from signal to natural frequency and mode shapes. Besides that, more than one tri-axial accelerometer is used to increase the tri-axial sensitivity on different points and the sensitivity of the tri-axial accelerometer is adjusted.

REFERENCES

- Brian, J. Schwarz & Mark, H. 1999. Experimental Modal Analysis
- Chee Kong Teo, 2002. Sensitivity Study Of A Truck Chassis, Master's Thesis, Mississippi State University, Department of Mechanical Engineering.
- Grube, Kris W. 1989. A Process for Investigating Geometric Sensitivity and Optimization of a Vehicle Structure, Ford Research Publication EM-89-1989.
- Halderman and Mitchell, 2001. Analysis and Optimization of Crankshafts Subject to Dynamic Loading
- Harris, C., Piersol, A., Harris Shock, 2002. Vibration Handbook, Fifth Edition, McGraw-Hill.
- Hieronimus and Klaus, 1977. A Few Aspects on the Development of Structural Models, SAE Technical Paper 770598.
- Jaidilson Jo da Silva, Antonio Marcus Nogueira Lima and Franz Helmut Neff, 2009. Vibration Analysis Based on Hammer Impact Test for Multilayer Fouling Detection.
- Jimin He and Zhi-Fang Fu, 2001. Modal Analysis.
- Kang, Y., Sheen G.J., Tseng M.H. 1997. Modal Analyses and Experiments for Engine Crankshaft. Journal of Sound and Vibration. Vol 214(3): 413-430. Article No. sv971512.
- Lee, C.K., Lin, C.T., Hsiao, C.C., and Liaw, W.C. 1998. New Tools for Structural Testing: Piezoelectric Impact Hammers and Acceleration Rate Sensors.
- Marc Halpern, 1997. Industrial Requirements and Practices in Finite Element Meshing: A Survey of Trends.
- Mazlan Zubair, Norsham Amin and Roslan Abd Rahman, 2003. Finite Element Modeling, Correlation and Model Updating of Stiffened Plate.
- McLaren-Mercedes, 2006. Vodafone McLaren-Mercedes: Feature - Stress to impress. Retrieved on 2006-10-03.

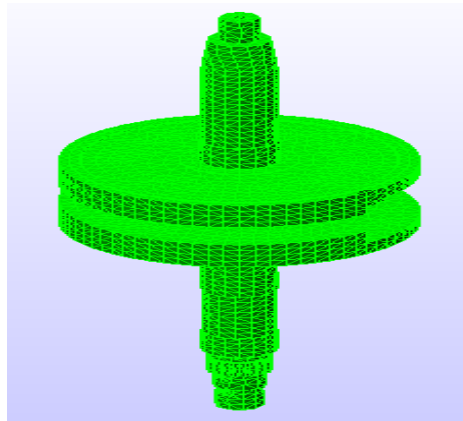
- Miomir Jovanovic, 2010. Accuracy of the FEM Analyses in the Function of the Finite Element Type Selection.
- Sani, M.S.M. and Nurba, N. 2007. Dynamics Modal Testing of Fun Kart Chassis.
- Simonovskia, LeonCizelj, NikolaJaksicb, 2010. The Influence of Finite Element Meshes on the Results of a Spatial Polycrystalline Aggregate Model.
- Turner, M.J., Clough, R.W., Martin, H.C., and Topp L.C. 1956. Stiffness and Deflection Analysis of Complex Structures. *Journal of the Aeronautical Sciences* 23: 805-824.
- Uhl, T., Lisowski, W., Mendrok, K., Kurowski, P. 2004. New Solutions in Experimental Modal Analysis of Mechanical Structures.
- Willard W. Pulkrabek, 2004. *Internal Combustion Engine*, Second Edition.
- William H. Crouse, Donald L. Anglin, 1993. *Piston Engine Operation*, *Automotive Mechanics* (115-116), Tenth Edition.
- Xavier BOURDIN, 2002. Comparison of Tetrahedral and Hexahedral Meshes for Organ Finite Element Modeling, an Application to Kidney Impact.
- Zissimos Mourelatos, P. 2001. A Crankshaft System Model for Structural Dynamic Analysis of Internal Combustion Engines.

APPENDIX A

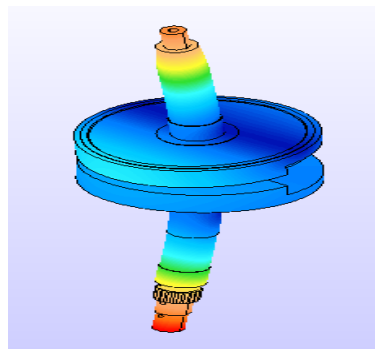
SIMULATION RESULT IN DIFFERENT MESH SIZE

2nd Simulation

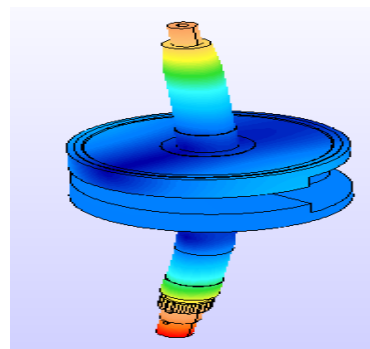
Mesh Aspect Ratio : 90%
Final Mesh Size : 3.94637mm
Total Element Create : 8878
Element type : Tetrahedron



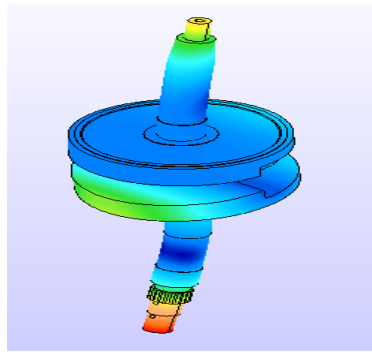
Mesh model 2nd Simulation



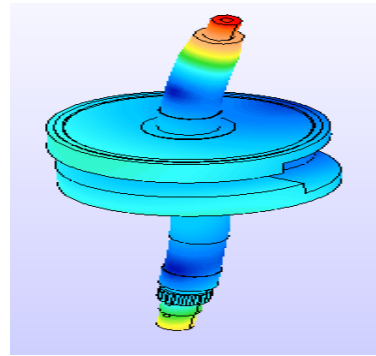
Mode shape 1



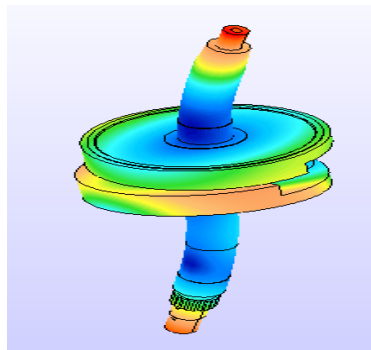
Mode shape 2



Mode shape 3



Mode shape 4



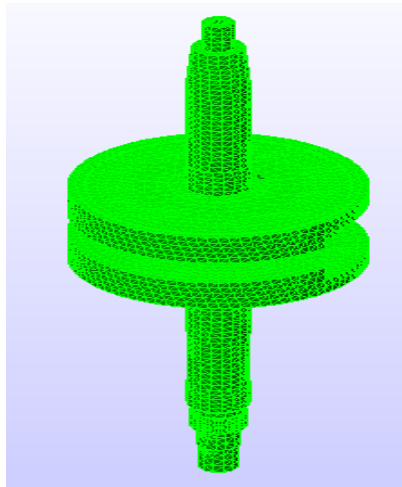
Mode shape 5

Figure 1: Second simulation**Table:** Frequency of 2nd simulation

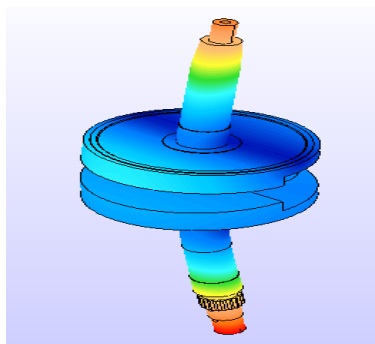
Mode Shape	Frequency (Hz)	Deflection Type
1	1128.73	Bending In face off
2	1276	Bending In face axis
3	2207	Bending out of face
4	2288.33	Bending out of face
5	2754.11	Bending out of face

3rd Simulation

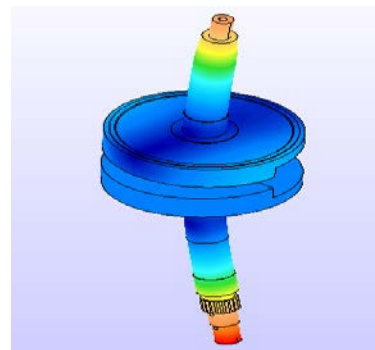
Mesh Aspect Ratio : 80%
Final Mesh Size : 3.22341 mm
Total Element Create : 12054
Element type : Tetrahedron



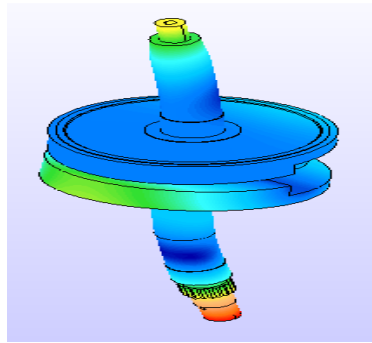
Mesh model 80%



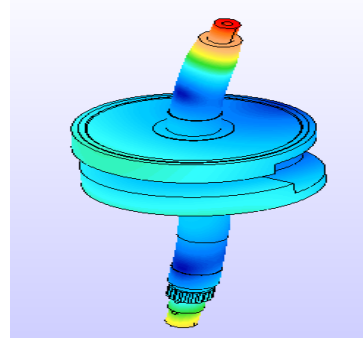
Mode shape 1



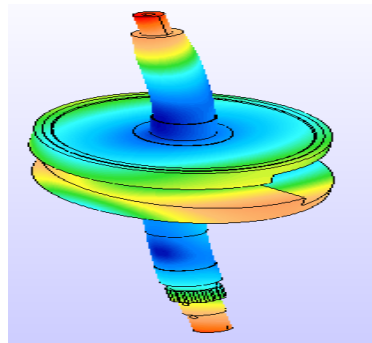
Mode shape 2



Mode shape 3



Mode shape 4



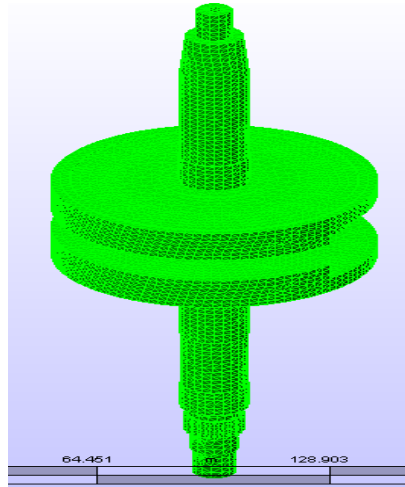
Mode shape 5

Figure 2: Third simulation**Table:** Frequency of 3rd simulation

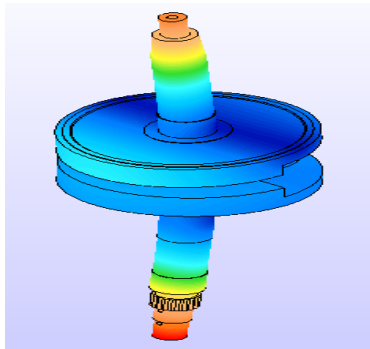
Mode Shape	Frequency (Hz)	Deflection Type
1	1106.17	Bending In face off
2	1252.73	Bending In face axis
3	2174.52	Bending out of face
4	2245.92	Bending out of face
5	2705.7	Bending out of face

4th Simulation

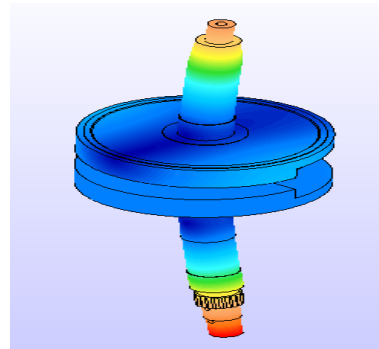
Mesh Aspect Ratio : 70%
Final Mesh Size : 2.57162 mm
Total Element Create : 18140
Element type : Tetrahedron



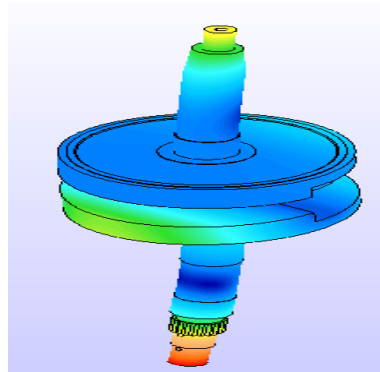
Mesh model 70%



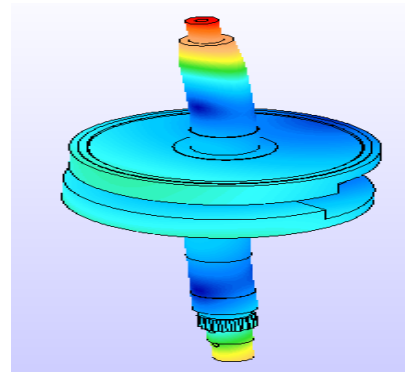
Mode shape 1



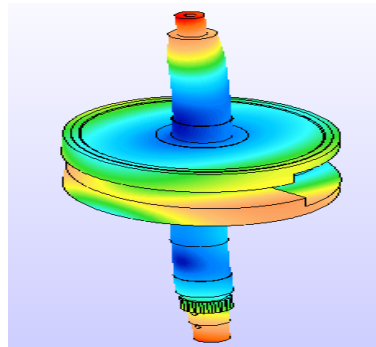
Mode shape 2



Mode shape 3



Mode shape 4



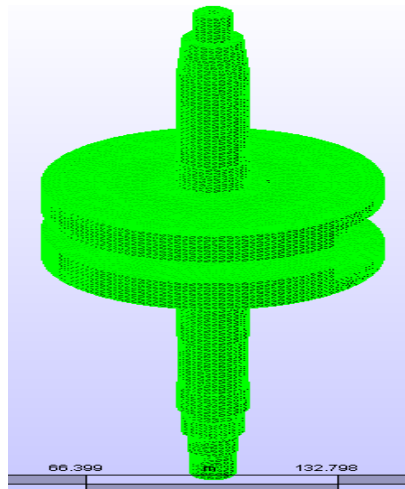
Mode shape 5

Figure 3: Fourth simulation**Table:** Frequency of 4th simulation

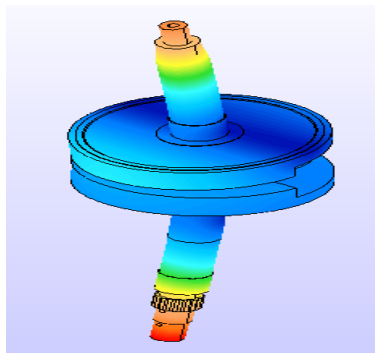
Mode Shape	Frequency (Hz)	Deflection Type
1	1086	Bending In face off
2	1231.99	Bending In face axis
3	2144.12	Bending out of face
4	2217.83	Bending out of face
5	2674.34	Bending out of face

5th Simulation

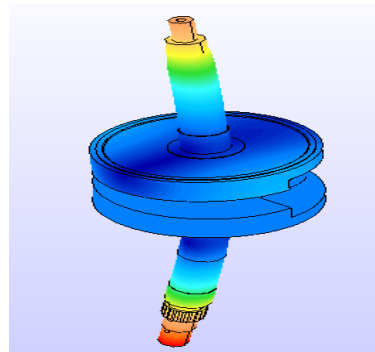
Mesh Aspect Ratio : 60%
Final Mesh Size : 1.48135 mm
Total Element Create : 49894
Element type : Tetrahedron



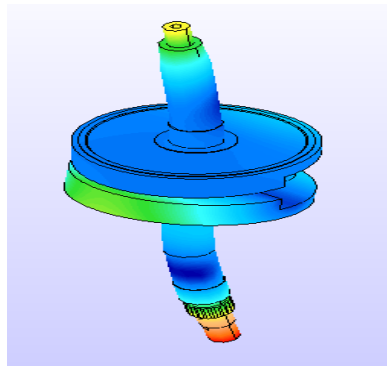
Mesh model 60%



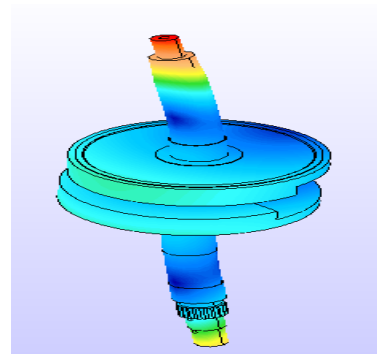
Mode shape 1



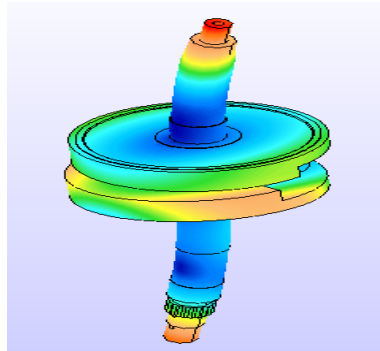
Mode shape 2



Mode shape 3



Mode shape 4



Mode shape 5

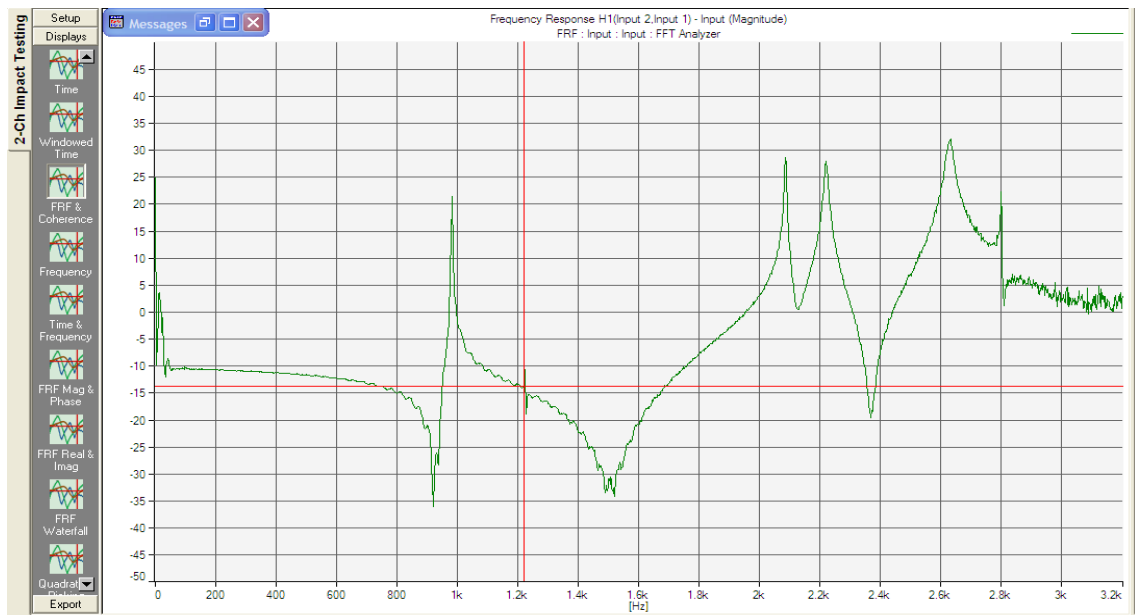
Figure 4: Fifth simulation**Table:** Frequency of 5th simulation

Mode Shape	Frequency (Hz)	Deflection Type
1	1059.6	Bending In face off
2	1204.59	Bending In face axis
3	2104.59	Bending out of face
4	2174.66	Bending out of face
5	2624.24	Bending out of face

APPENDIX B

EXPERIMENT RESULTS AT DIFFERENT POINT ON CRANKSHAFT

2nd Point

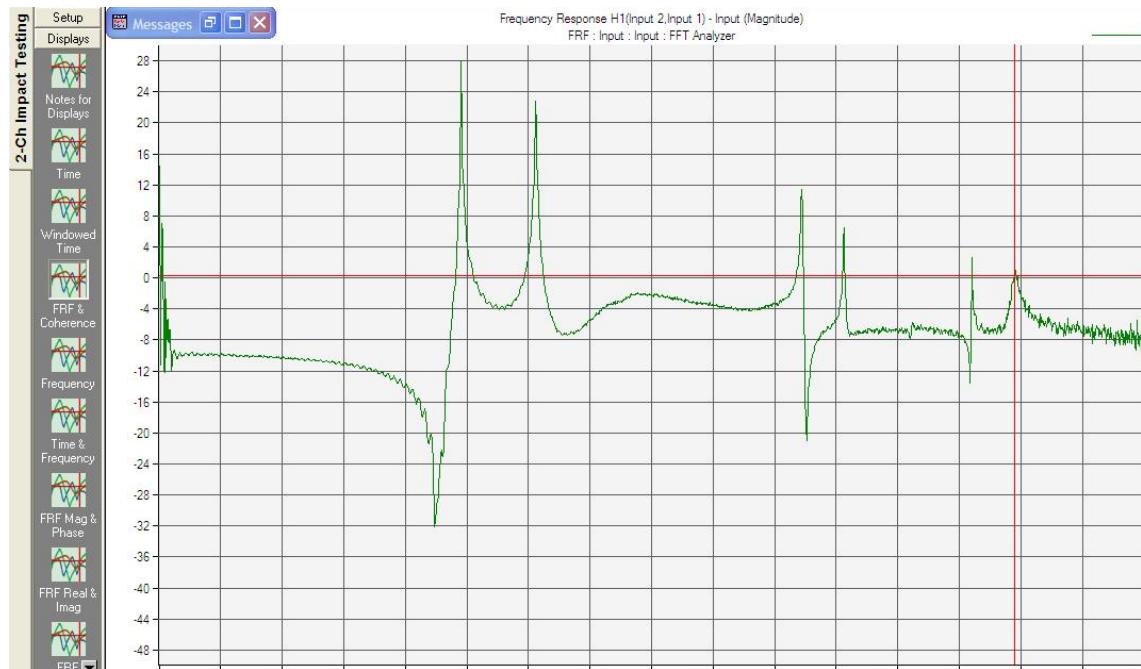


Frequency measured at point 2

Table: Value of Natural Frequency in different Mode Shape at point 2

Mode Shape	Frequency (Hz)	Damping ratio
1	990	0.177
2	1224	0.256
3	2084	0.132
4	2218	0.243
5	2798	0.059

3rd Point

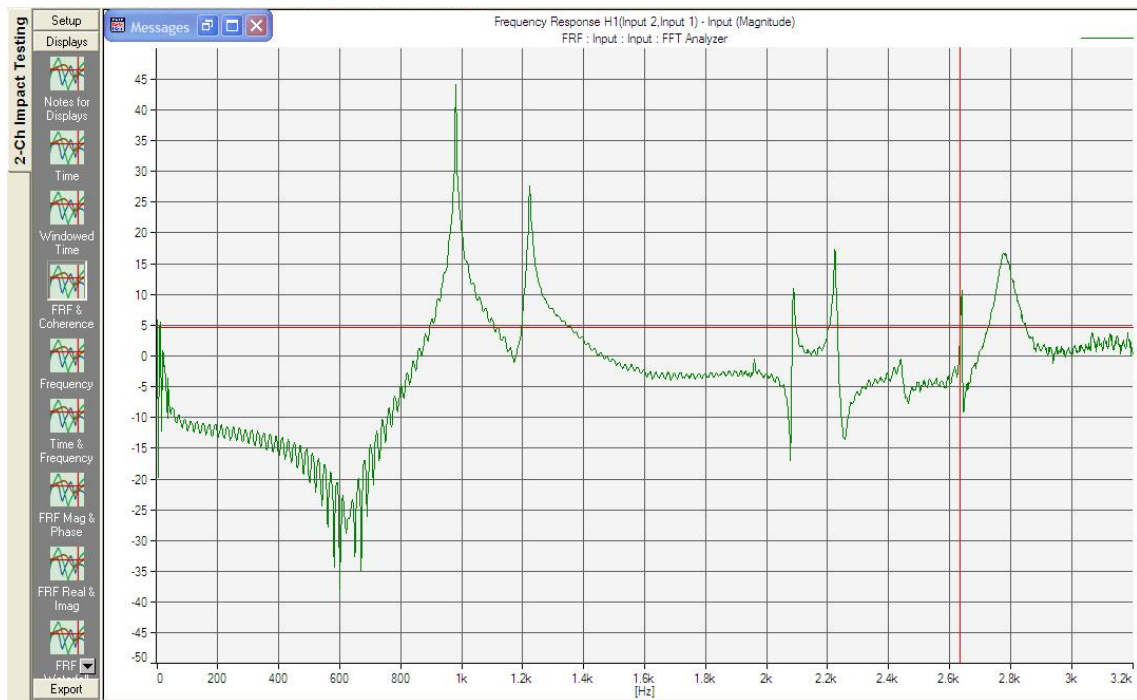


Frequency measured at point 3

Table: Value of Natural Frequency in different Mode Shape at point 3

Mode Shape	Frequency (Hz)	Damping ratio
1	990	0.111
2	1224	0.16
3	2084	0.12
4	2218	0.18
5	2798	0.552

4th Point

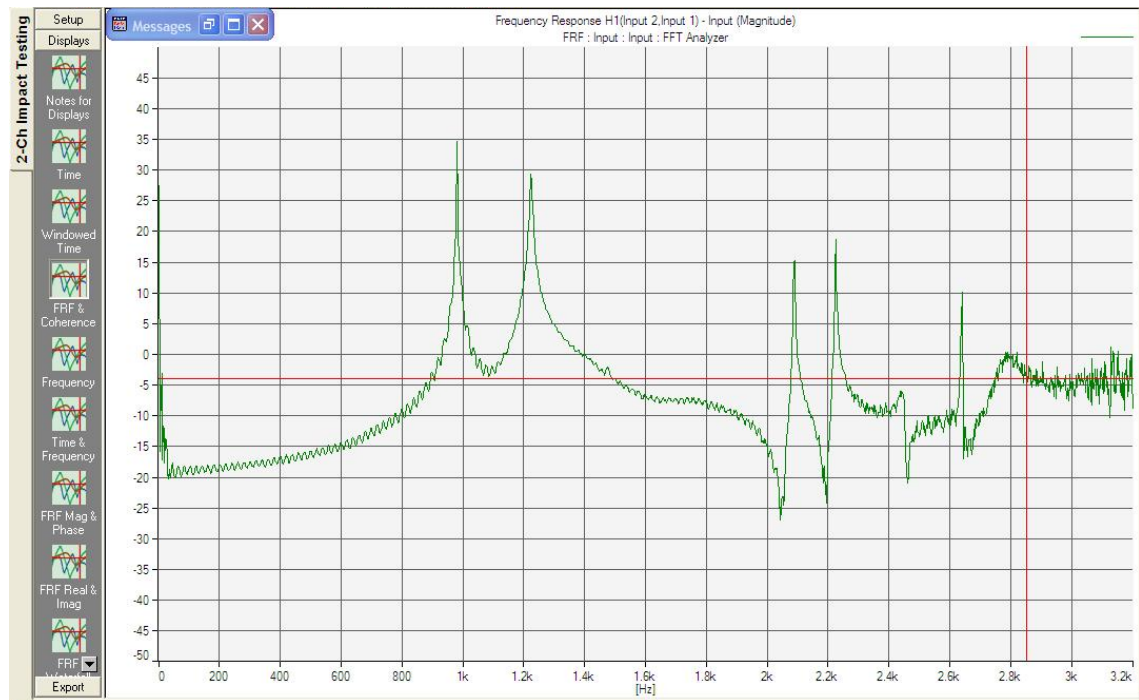


Frequency measured at point 4

Table: Value of Natural Frequency in different Mode Shape at point 4

Mode Shape	Frequency (Hz)	Damping ratio
1	990	0.199
2	1222	0.253
3	2086	0.126
4	2224	0.142
5	2782	0.064

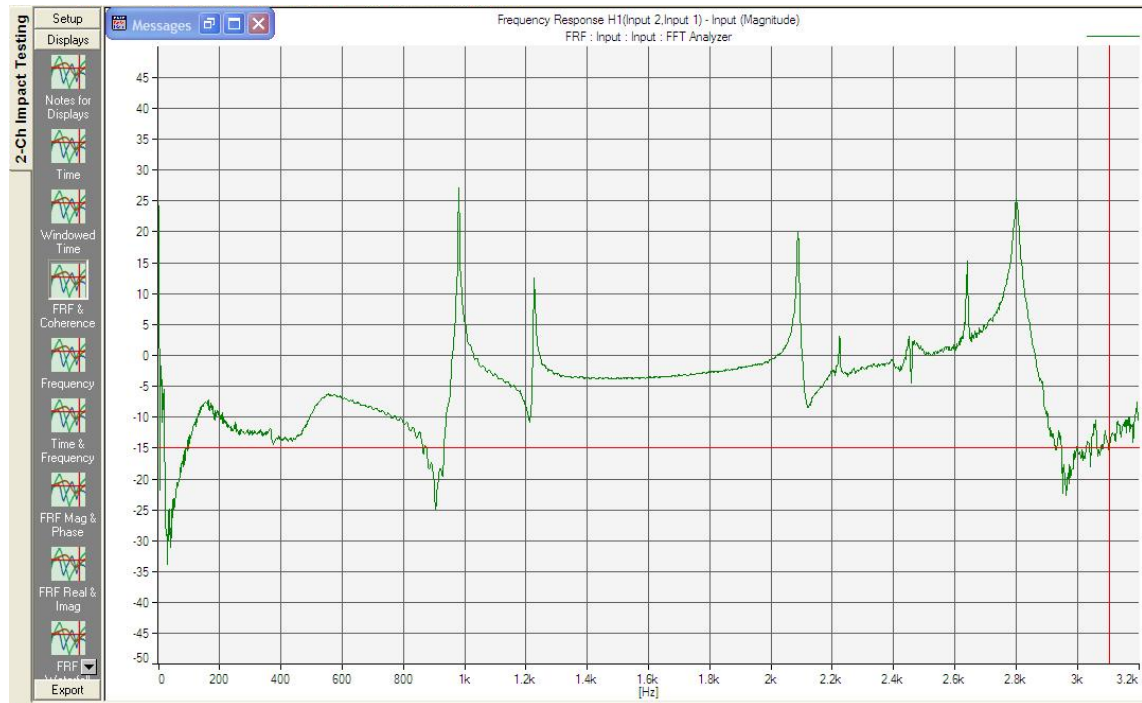
5th Point



Frequency measured at point 5

Table: Value of Natural Frequency in different Mode Shape at point 5

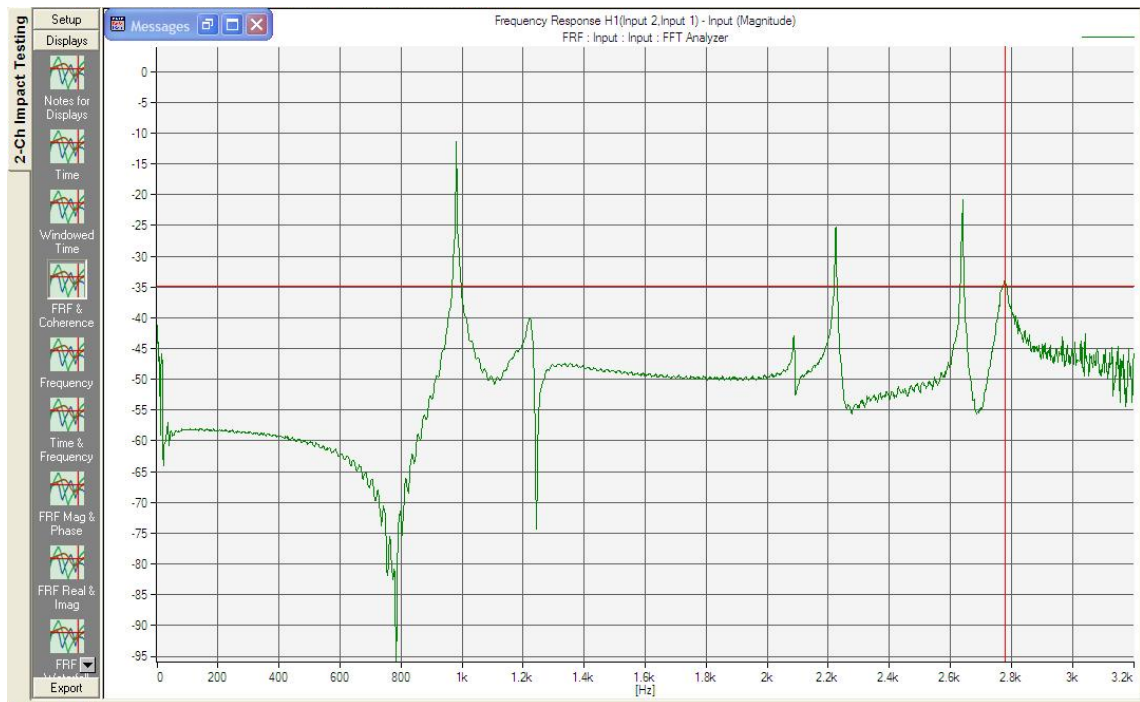
Mode Shape	Frequency (Hz)	Damping ratio
1	990.12	0.129
2	1224	0.302
3	2082	0.109
4	2216	0.056
5	2798	0.048

6th Point

Frequency measured at point 6

Table: Value of Natural Frequency in different Mode Shape at point 6

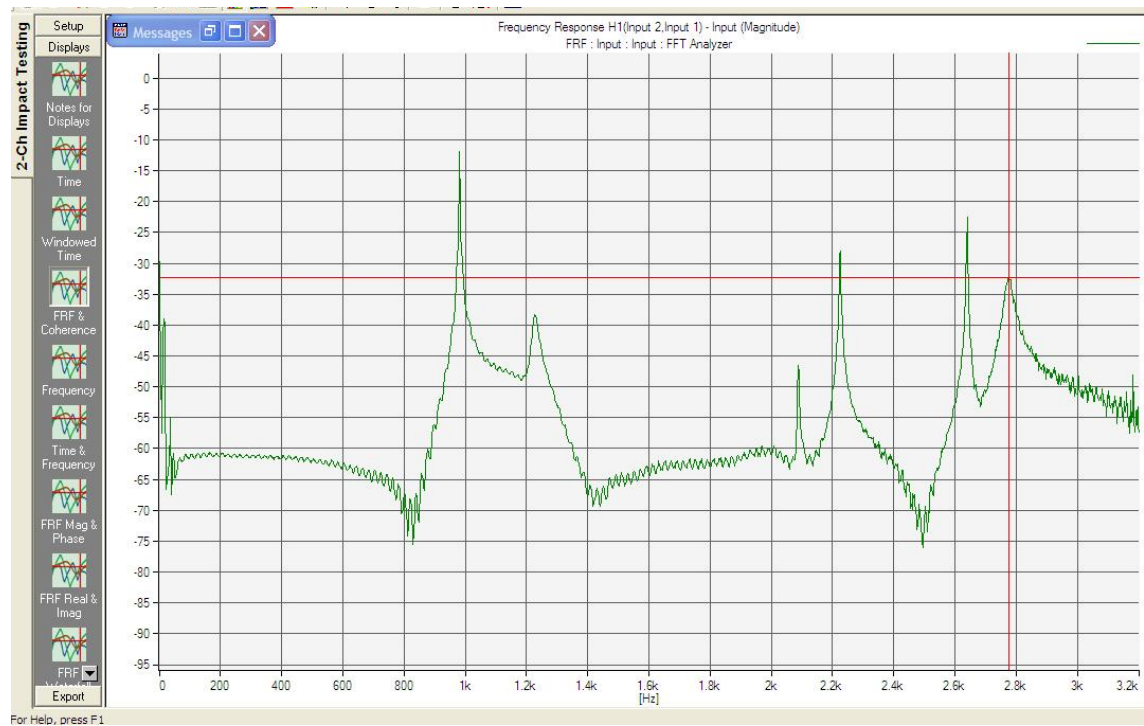
Mode Shape	Frequency (Hz)	Damping ratio
1	990	0.199
2	1226	0.163
3	2086	0.117
4	2222	0.144
5	2800	0.205

7th Point

Frequency measured point 7

Table: Value of Natural Frequency in different Mode Shape at point 7

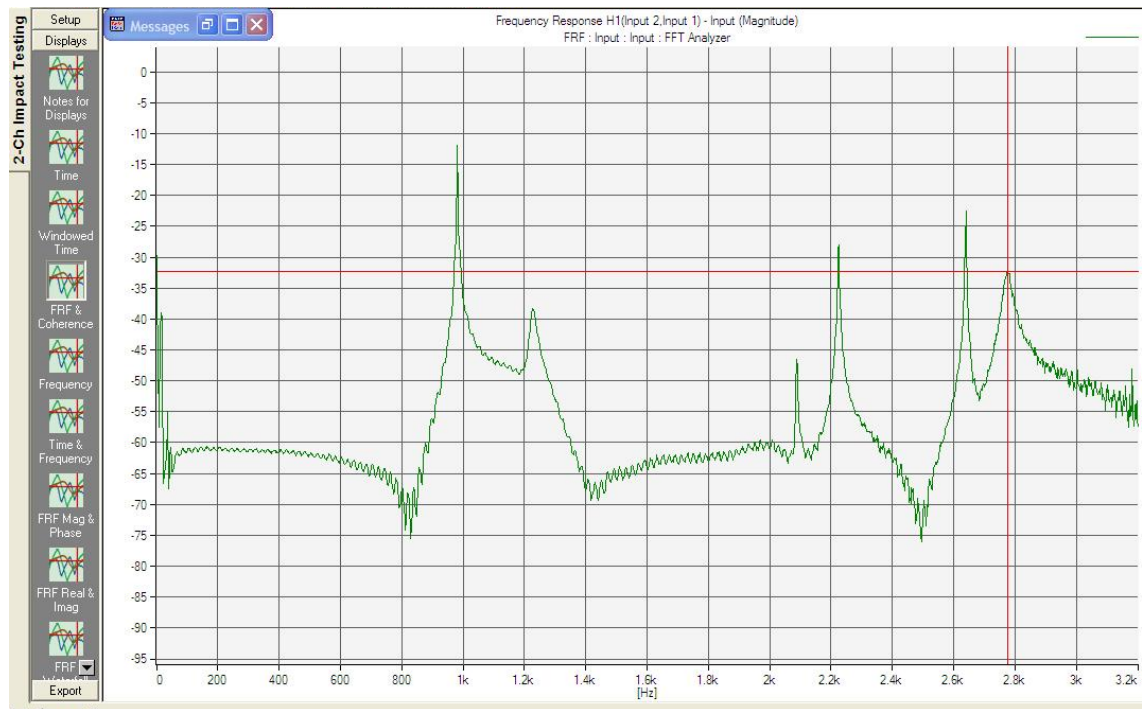
Mode Shape	Frequency (Hz)	Damping ratio
1	990	0.11
2	1226	0.935
3	2086	0.165
4	2222	0.104
5	2800	0.507

8th Point

Frequency measured point 8

Table: Value of Natural Frequency in different Mode Shape at point 8

Mode Shape	Frequency (Hz)	Damping ratio
1	990	0.14
2	1220	0.865
3	2086	0.109
4	2224	0.113
5	2776	0.0477

9th Point

Frequency measured point 9

Table: Value of Natural Frequency in different Mode Shape at point 9

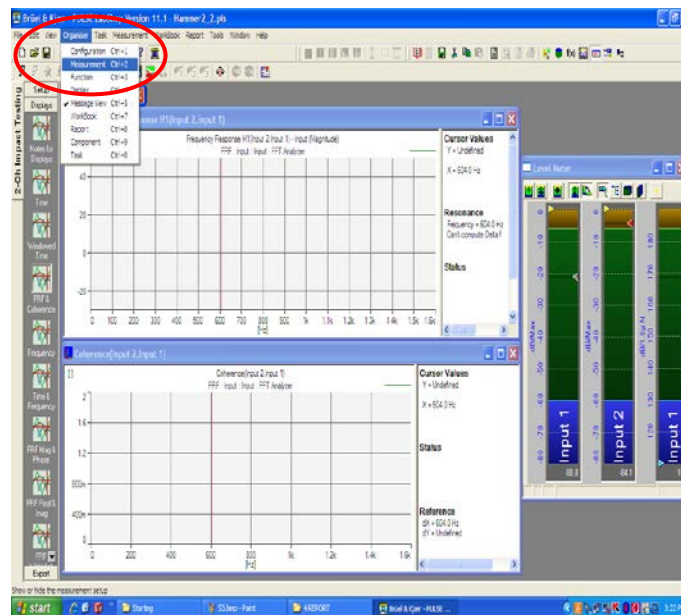
Mode Shape	Frequency (Hz)	Damping ratio
1	990	0.16
2	1226	0.765
3	2086	0.129
4	2224	0.115
5	2776	0.048

APPENDIX C

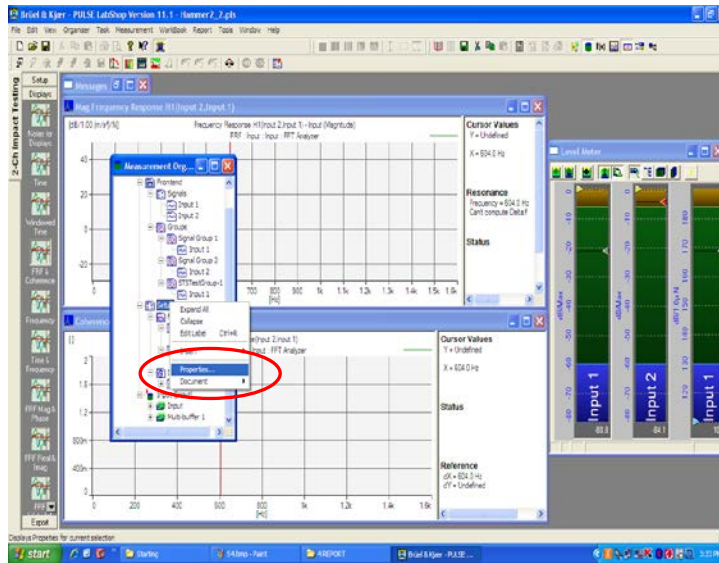
PROCEDURES TO RUN THE PULSELAB SOFTWARE

There are several steps that are used to conduct this experiment:-

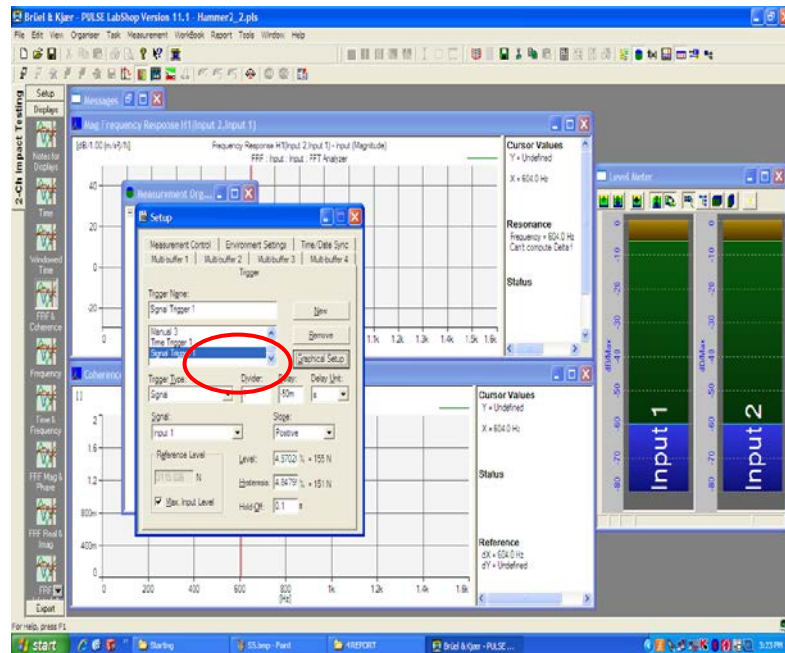
- I. PULSE LabShop version 11.1-hammer 2_2 is opened.
- II. On the top toolbar, 'Organiser' is chosen and 'measurement' has been clicked.



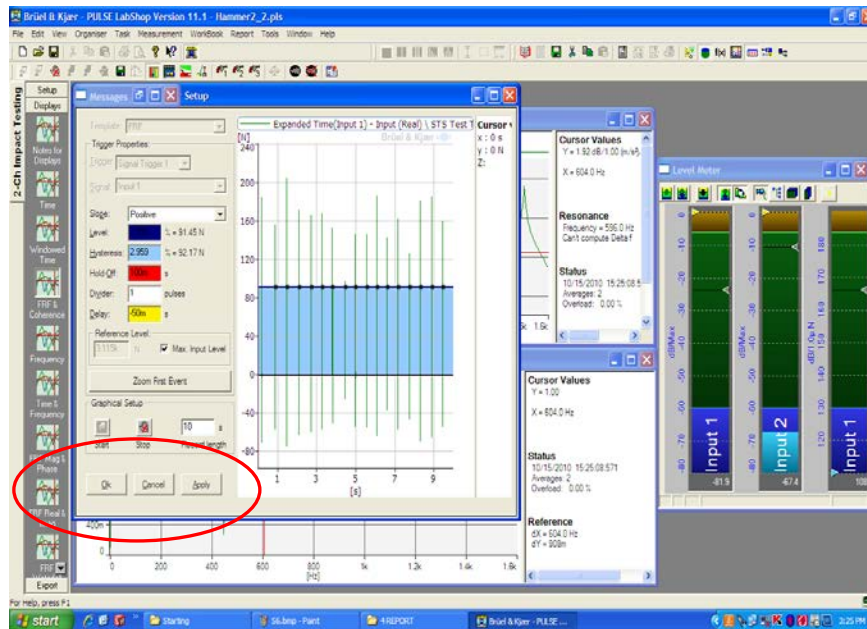
- III. Measurement Organiser tab will be appears. Then, right click at 'Setup' and 'Properties'. has chosen



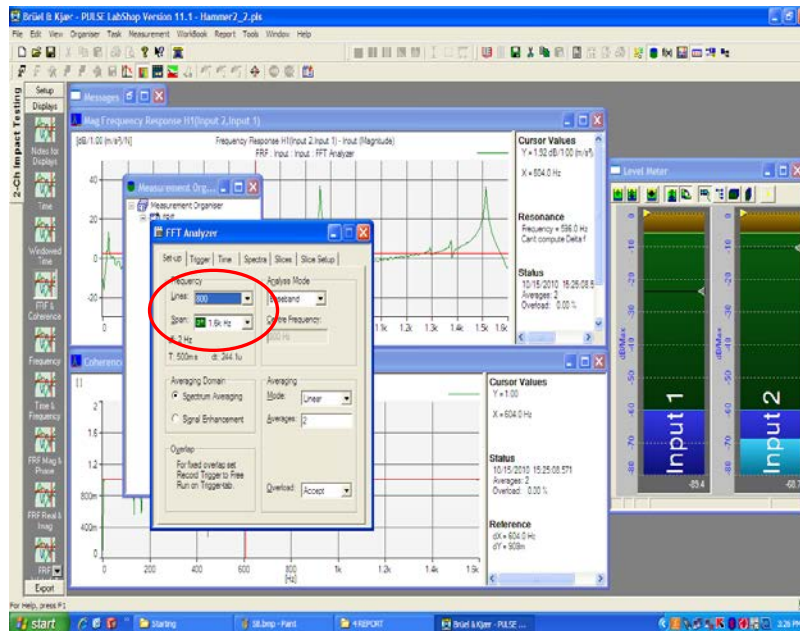
- IV. Setup tab will appear. The 'Graphical Setup' button has been clicked on.



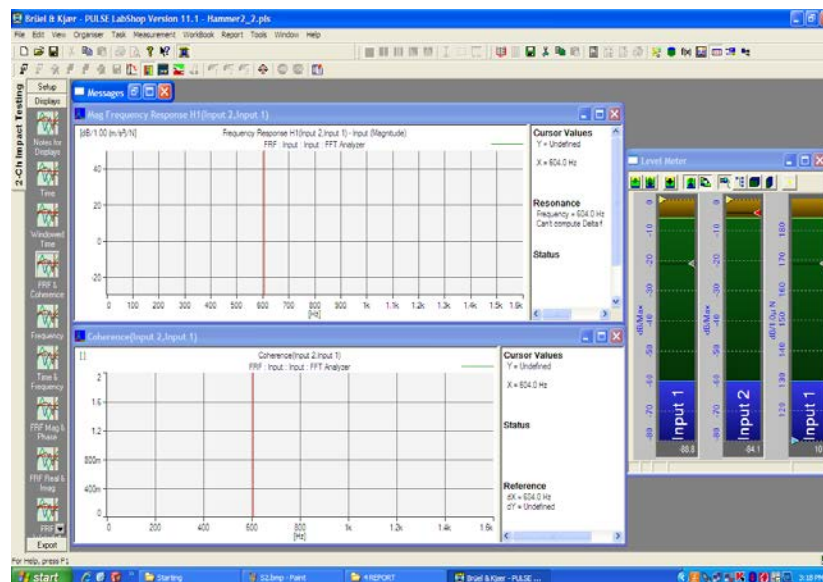
- V. At the 'Record Length' option is been set to 10 seconds. The 'Start' button has been click, then force is applied to work piece using hammer. After 10 seconds, 'Stop' button is been click. The graph will appear like figure above. After that, 'Apply' button has been clicked and then 'Ok'.



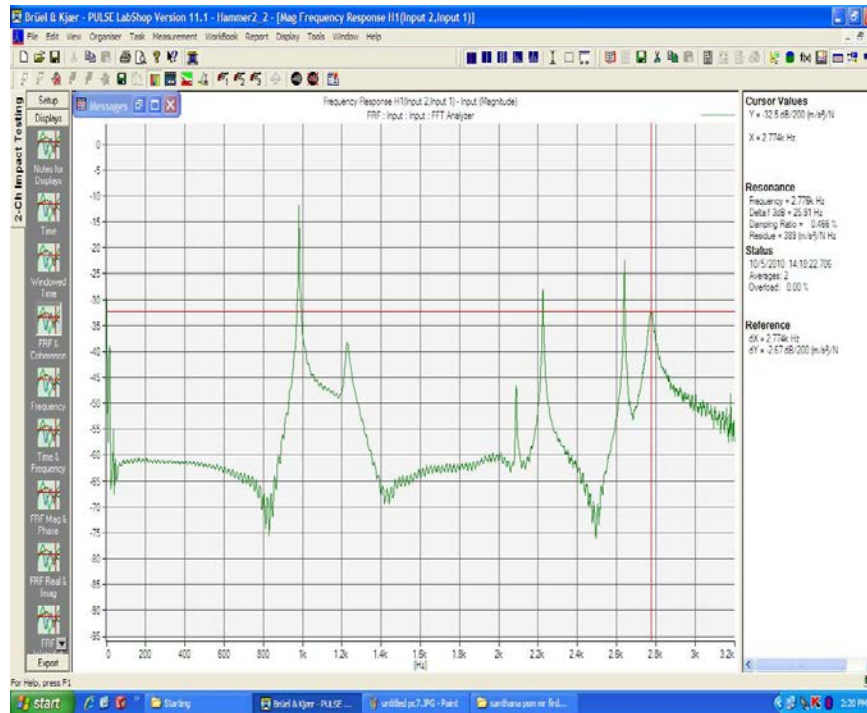
- VI. At Measurement Organiser tab, right click at 'FFT Analyzer' then 'Properties' has been chosen.
- VII. 'FFT Analyzer' tab will appear. At Setup options, suitable 'Lines' and 'Span' has been chosen to obtain perfect graph shape.



VIII. At the left side toolbar, ‘Displays’ is been clicked and ‘FRF & Coherence’ options has been chosen. Then the software will show both Frequency Response H1 and Coherence graph. “Level Meter” tab shows input 1 that represent hammer and input 2 that represent accelerometer



- IX. Then 'start measurement' button has been clicked in order to run the software.
- X. Then FRF graph will display



- XI. From this graph, the value of Natural Frequency can be obtained.

APPENDIX D

GANTT CHART / PROJECT SCHEDULE FOR FYP 1

NO.	TASK	Week														
		1	2	3	4	5	6	7	8	9	10	11	12	13	14	15
1	Receiving Title	Planning	Actual													
2	Receiving objective and scope briefing from Sva		Planning	Actual												
3	Introduction			Planning	Actual											
4	Literature review			Planning	Actual				Planning							
5	Defining material								Planning	Actual						
6	CAD modelling				Actual					Planning						
7	Finite element analysis							Actual			Planning					
8	Methodology								Planning	Actual						
9	Tabulation and compilation of result and data													Actual		
10	Slides preparation and presentation														Actual	Planning
11	Report Submission															Actual

	Planning
	Actual

GANTT CHART / PROJECT SCHEDULE FOR FYP 2

